Green Chemistry

ROYAL SOCIETY OF CHEMISTRY

CRITICAL REVIEW

View Article Online
View Journal | View Issue

Cite this: *Green Chem.*, 2025, **27**, 10372

Sustainable synthesis of nitrogen-containing chemicals from biomass-derived carbonyls: catalytic strategies and mechanistic perspectives in multicomponent systems

Zhisen He,[a,b] Shanjian Liu,[a] Fernando Cardenas-Lizana,[b] Dongmei Bi *[a] and Aimaro Sanna *[b]

Nitrogen-containing chemicals (NCCs) are widely used in pharmaceuticals, agrochemicals, polymers, and fine chemicals. Traditional synthesis methods, based on fossil resources, pose sustainability and environmental challenges. Biomass and its derived carbonyl compounds (aldehydes, ketones), with high reactivity and structural diversity, show great potential in catalyzed amination/ammoniation for NCCs. Due to the limited systematic experimental studies on the competitive reaction mechanisms in complex multicomponent systems, there is a lack of understanding of the multicomponent reaction characteristics of biomass-derived aldehydes and ketones. By comparing the regulatory advantages and limitations of different catalytic systems in a multi-functional group environment, this review aims to identify the key factors influencing the competition and selectivity of nitrogen conversion pathways in aldehyde/ketone platform compounds. It focuses on key reaction mechanisms and strategies to control competing pathways in thermochemical conversion. It provides an in-depth analysis of the performance differences between homogeneous and heterogeneous catalysts in directed conversion. It also seeks to highlight the research priorities that need to be addressed in complex systems, based on existing reaction trends. Despite significant progress in optimizing reaction efficiency and selectivity, challenges remain in industrial applications. These include the complex functional group characteristics of biomass-derived aldehydes and ketones, system diversity, catalyst stability, and product separation costs. Future research should focus on the precise design of multifunctional catalysts, dynamic analysis of reaction pathways, and the development of multiscale reaction-separation coupling technologies. This review aims to promote the sustainable synthesis and large-scale application of biomass-based NCCs, supporting the low-carbon economy transition.

Received 5th June 2025,
Accepted 5th August 2025

DOI: 10.1039/d5gc02853a

rsc.li/greenchem

Green foundation

1. This review highlights recent progress in the green catalytic synthesis of nitrogen-containing chemicals (NCCs) from biomass-derived aldehydes and ketones, emphasizing mechanistic insights into competitive pathways in multicomponent systems.
2. The valorization of biomass carbonyls for nitrogen incorporation addresses the urgent need for renewable feedstocks in chemical manufacturing, making this area of wide relevance for sustainable materials, pharmaceuticals, and fuels.
3. Future advances lie in designing multifunctional catalysts and coupling kinetic modeling with reaction-separation strategies. The insights provided will help direct greener, more selective nitrogen conversion processes and broaden the impact of green chemistry in biomass utilization.

1. Introduction

Nitrogen-containing heterocyclic compounds (NHCs) play a central role in fine chemicals, serving as key structural motifs in a wide range of pharmaceuticals and agrochemicals, with substantial annual demand.[1] For example, pyridine-based agrochemicals—recognized as the fourth generation of pesticides—offer advantages such as high efficacy, low toxicity, and

[a]*School of Agricultural Engineering and Food Science, Shandong Research Center of Engineering & Technology for Clean Energy, Shandong University of Technology, Zibo 255000, China. E-mail: dongmei070719@163.com*
[b]*Institute of Mechanical, Process and Energy Engineering, School of Engineering and Physical Sciences, Heriot-Watt University, Edinburgh EH14 4AS, UK. E-mail: A.Sanna@hw.ac.uk*

environmental compatibility. In addition, certain pyrrole derivatives exhibit strong fluorescence properties,[2] making them valuable in energy-related applications such as electroluminescent materials. However, most NHCs are currently synthesized industrially from fossil-based feedstocks through multi-step processes, which are often complex and generate substantial pollutant emissions.[3] Studies have shown that, compared to petroleum-based hydrocarbons, biomass and its derivatives are more amenable to nitrogen incorporation, offering a promising route for the sustainable production of NHCs.[4] Therefore, the thermochemical conversion of biomass and its derivatives to high-value NHCs is of great significance.

Agricultural and forestry biomass, as the only renewable carbon source capable of producing liquid, gaseous, and solid fuels as well as high-value chemicals, offers advantages such as low cost, wide availability, and abundant reserves. It plays a vital role in the production of energy, pharmaceuticals, and catalyst supports. However, it should be emphasized that when utilizing the product as fuel, the removal of oxygenated compounds and stringent control of nitrogen content must be addressed to comply with specific fuel standards. For instance, jet fuel applications require maintaining extremely low nitrogen levels, thereby enhancing the overall quality of the bio-oil. In particular, its diverse functional groups are increasingly viewed as a promising alternative for the green synthesis of nitrogen-containing chemicals (NCCs). Biomass-derived intermediates also exhibit good reactivity in C–N bond formation. Since the concept of producing NHCs from biomass and its derivatives was first proposed, many researchers, including our group, have successfully synthesized various NHCs and continue to focus on improving their selectivity.[5,6] However, the coexistence of multiple functional groups and components also leads to challenges such as poor product selectivity and numerous side reactions. The complexity and low selectivity of NHCs in the product mixture significantly limit their further application and development.

Although industrial production faces evident issues such as high emissions, high costs, and non-renewable feedstocks, NHCs are still mainly produced from fossil resources and organic synthesis in the chemical industry. For instance, the aldehyde/ketone–ammonia method typically employs reactive carbonyl compounds such as aldehydes and ketones.[7] It is noteworthy that biomass primary pyrolysis derivatives contain a significant amount of aldehyde and ketone compounds. Our previous research has shown that during the nitrogen-rich pyrolysis of biomass, aldehyde and ketone intermediates serve as precursors for the nitrogenation conversion into NHCs.[5] Unlike petroleum-based feedstocks, biomass-derived aldehydes and ketones (*e.g.*, furfural (FF), 5-hydroxymethylfurfural (HMF)) offer high reactivity and structural diversity for efficient C–N bond formation.[8,9] Xu *et al.* exploited the high reactivity of biomass-based furfural to develop an intramolecular cycloaromatization strategy, directly upgrading furfural to renewable isoindolinones.[10] Leveraging these advantages, growing research has focused on catalytic amination of biomass-derived molecules as a green strategy for C–N bond construction. Yan *et al.*[11] provided a detailed overview of recent advances in the selective synthesis of NHCs from various biomass-derived compounds using transition metal catalysts. Zhong *et al.*[12] focused on the catalytic amination of biomass-derived model compounds such as HMF, FF, and acetylpropionic acid. The review highlights advances in novel catalysts and the mechanistic understanding of intermediates, emphasizing structure–activity relationships. Zhao *et al.*[13] focused on FF as a feedstock and highlighted recent advances in heterogeneous catalytic systems for its selective transformation. These reviews are more focused on the field of organic chemical synthesis of biomass derivatives. They often require high-quality primary reactants, involve harsh conditions, and have limited applicability in multicomponent reactions. In biomass-derived aldehyde/ketone systems, the presence of multiple functional groups poses significant challenges. The selective conversion of a single functional group using a specific noble metal catalyst is often inadequate for the efficient production of NHCs.[14] Excessive hydrogenation activity of certain noble metal catalysts can lead to over-hydrogenation of various carbonyl groups, resulting in poor chemoselectivity toward the desired target products.[15]

Zhisen He

Zhisen He is currently a joint Ph. D. student at Heriot-Watt University and a doctoral candidate at Shandong University of Technology. His research focuses on the production of liquid fuels and high-value fine chemicals from biomass and its oxygenated derivatives, with particular interest in nitrogen-containing compounds.

Shanjian Liu

Shanjian Liu is a Professor in the School of Agricultural Engineering and Food Science, Shandong University of Technology. His research interests focus on clean energy utilization technology. Fields of interests are directed thermal conversion technology of biomass, biomass/coal clean and efficient combustion technology utilization technology of new energy solid waste, and new energy integrated system modeling.

It is evident that most of these reviews focus on specific catalytic systems, such as transition metal-catalyzed amination, high-value utilization of FF, or organic synthesis of specific reaction pathways from simple model compounds to five- or six-membered heterocycles. Although some reviews provide comprehensive insights into specific catalytic conversion techniques, they lack an understanding of the multicomponent reaction characteristics of biomass and its derived aldehydes and ketones. Moreover, our previous review focused on the early-stage research of NCCs production from biomass thermochemical conversion.[16] It was limited to a qualitative summary of the general pyrolysis behaviors and transformation mechanisms by which broad-spectrum feedstocks yield NCCs. The emphasis was placed on the diversity of raw materials, the macroscopic patterns of pyrolysis behavior, and the overall characteristics of product composition. This is largely due to the limited experimental research on the competitive mechanisms of reaction pathways in complex multicomponent systems. Currently, knowledge on reaction selectivity control, catalyst directional design, and the synergistic mechanisms of multifunctional groups remains fragmented.

To narrow this knowledge gap, this review attempts to construct a systematic mechanistic framework based on existing mechanism analysis, catalysis, and reaction kinetics perspectives. By comparing the regulatory advantages and limitations of different catalytic systems in a multi-functional group environment, this review aims to identify the key factors influencing the competition and selectivity of nitrogen conversion pathways in aldehyde/ketone platform compounds. It also seeks to highlight the research priorities that need to be addressed in complex systems, based on existing reaction trends. Building on our previous review work, it represents a shift from qualitative summaries at the feedstock–product level to in-depth mechanistic analysis at the molecular level. To achieve this goal, the review first outlines the sources and nitrogenation potential of aldehyde/ketone platform compounds in biomass (section 2). Section 3 systematically discusses their reaction characteristics and research progress in typical reactions such as reductive amination, amination, and cyclization. The analysis of reaction pathway competition in multicomponent systems, combining thermodynamic and kinetic modeling, reveals the control of energy barriers in key reaction steps and strategies for suppressing side reactions (section 4). Section 5 focuses on the coupling relationship between catalyst types, active site structures, and system selectivity, based on literature and experimental studies. Finally, section 6 summarizes current challenges and future development directions to promote the efficient and green conversion of biomass-derived aldehyde/ketone platform compounds into high-value NHCs.

2. Production applications and limitations of biomass-derived NHCs

2.1 Feedstock selection and utilization

2.1.1 Biomass-derived platform compounds. Biomass-derived platform compounds (such as furan, FF, HMF, glucose, polylactic acid, glycerol, *etc.*) are obtained from natural biomass through primary conversion processes. Their well-defined molecular structures and rich functional groups make them ideal intermediates for the efficient production of NHCs (Fig. 1). Although research on the use of biomass-derived platform compounds in pyrolysis for producing high-value NHCs is relatively limited, numerous studies on biomass-based production of NHCs have directly or indirectly demonstrated that platform compounds derived from primary biomass pyrolysis, which are not separated from the reaction products, may serve as precursors or reaction intermediates for the final target NHCs. In previous studies on nitrogen-rich biomass pyrolysis, it was found that the carbonyl compounds produced, especially aldehydes and ketones, are highly prone to conversion into NHCs through various reactions.[17,18] Under non-catalytic conditions, the conversion ratios of bio-oil com-

Fernando Cardenas-Lizana

Fernando Cárdenas-Lizana is an Assistant Professor at Heriot-Watt University. Prior to this, he was a Research Scientist at the Swiss Federal Institute of Technology (EPFL) Lausanne and Doctoral Assistant in UK. The main topics of his research are design of new generation colloidal supported and bulk catalytic materials, characterisation techniques as a tool to obtain fundamental molecular-level mechanistic information, selective hydrogenation/hydrogenolysis reactions and kinetic modelling.

Dongmei Bi

Dongmei Bi is a Professor in the School of Agricultural Engineering and Food Science, Shandong University of Technology. Her interests are high-value utilization technology of biomass, and preparation of catalysts for pyrolysis. Fields of interests are biomass catalytic pyrolysis mechanism and regulation technology, biomass syngas preparation technology, and organic solid waste resource utilization technology.

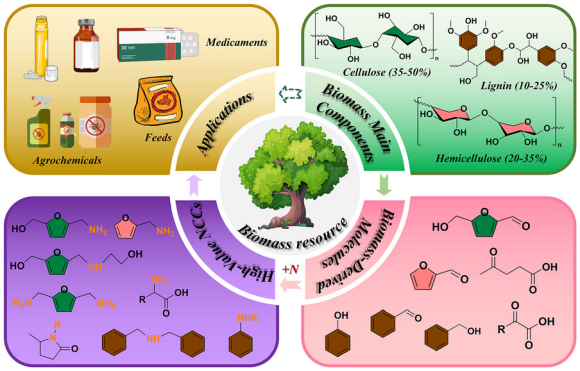

Fig. 1 Efficient conversion of natural biomass into high-value NCCs: thermochemical conversion pathway.

ponents to NHCs are: ketones > aldehydes > furans > phenols > esters > alcohols. Biomass-derived platform compounds possess rich functional groups and high chemical reactivity, making them key precursors for exploring the synthesis of NHCs. FF, with its furan ring and aldehyde group structure, stands out, and can efficiently generate indole-like compounds in reactions with ammonia.[19] This transformation typically proceeds *via* the formation of a furfuryl imine intermediate, which undergoes cyclization and hydrogen transfer steps to generate furfurylamine (FAM) and subsequently indole derivatives. Studies have shown that under the influence of the HZSM-5 catalyst, FF undergoes multi-step reactions, including the formation of imine intermediates, cyclization, and cleavage, ultimately generating indole-like compounds.[20] Under pyrolysis conditions of 650 °C, the carbon yield of indole reaches as high as 20.79%, while the acidity of the catalyst's active sites plays a decisive role in regulating the reaction pathway.[21,22] As an important intermediate in the catalytic dehydration of glycerol, acrolein is widely used for synthesizing pyridine derivatives due to its high reactivity. In the ZnO/HZSM-5 composite catalytic system, acrolein reacts with ammonia through a condensation reaction to generate pyridine and its derivatives, with a total yield of up to 61.14%. ZnO primarily provides dehydrogenation functionality in this system, while HZSM-5 promotes the stability of intermediates and enhances selectivity.[18] The reaction pathway involves acrolein condensing with ammonia to form imine intermediates, followed by intramolecular rearrangement to yield pyridine-type compounds. In the direct reaction with glycerol, nano-HZSM-5, due to its high specific surface area and optimized pore distribution,[23] not only facilitates the reaction between glycerol and ammonia to produce pyridine derivatives but also reduces the formation of by-products. The carbon yield of glycerol conversion can reach 35.6%.[24] HMF, with its dual hydroxymethyl and aldehyde groups, exhibits unique advantages as a precursor for pyrrole-based compounds. Under acidic conditions, HMF typically forms Schiff base or 1,4-dicarbonyl intermediates, which then cyclize to yield pyrrole frameworks through a Paal–Knorr-type mechanism. Studies have shown that under acidic catalytic conditions, HMF undergoes a series of condensation and dehydration reactions to generate pyrrole or quinoline-type products, and the catalyst's pore size and surface acidity significantly influence the selectivity of NHCs.[25]

Compared to the direct utilization of natural biomass, research on derived platform compounds shows higher selectivity and reaction efficiency. However, studies have also pointed out that the industrialization of NHCs from derived platform compounds is still constrained by high costs and multi-functional catalyst systems. In most biomass-derived aldehyde/ketone systems, multiple functional groups are present, such as FF,[26] HMF,[27] benzaldehyde,[28] acetophenone,[29] *etc.*[30] Considering the selective conversion of a specific functional group with a single noble metal catalyst cannot fully apply to the production of NHCs from biomass. In organic chemical synthesis, achieving high chemical selectivity for a single target product is relatively easy. However, in the production of NHCs from biomass, excessive hydrogenation capability of a single or certain noble metal catalyst can lead to over-hydrogenation of multiple functional groups in the system, including furan, hydroxyl, aromatic, and imidazole groups. This results in unsatisfactory chemical selectivity for the single target product.[7,14,15] In particular, the coexistence of multiple reaction intermediates such as imines, enamines, and aldol adducts complicates the control over reaction direction and product selectivity in multicomponent systems.

2.1.2 Role of model compounds. Model compounds, in a sense, can also be considered as platform compounds derived from biomass (such as acetaldehyde, acetone, formaldehyde, *etc.*), but their primary role is to provide a key reference system for studying the complex biomass conversion processes. Compared to platform compounds, these model compounds have simpler and more defined structures, making it easier to track their reaction pathways and analyze intermediate products. For example, the reaction of acetone with ammonia in the presence of a ZnO catalyst has been confirmed to efficiently generate pyrrole compounds.[11] Additionally, acetaldehyde, when reacting with amines, can generate different NHCs by controlling reaction conditions, such as imidazole and pyridine derivatives.[31] These results provide valuable references

Aimaro Sanna

Aimaro Sanna is an Associate Professor in the School of Engineering and Physical Sciences at Heriot-Watt University, UK. His research primarily focuses on heterogeneous catalysis, as well as pyrolysis, gasification, and hydrogenation processes for biorefining. He is particularly interested in technologies for CO_2 capture and utilization, and in the valorization of waste materials to hydrogen.

for the actual biomass and biomass-derived platform compound conversion processes. The study of model compounds not only reveals the catalytic control over reaction pathways but also offers significant theoretical support for the optimization of complex biomass systems. The reaction outcomes of model compounds provide a data foundation for the development of high-selectivity and high-stability catalysts. This can further combine the multi-functional group characteristics of complex biomass and apply the theoretical findings from model compounds to the collaborative optimization of multi-step reaction pathways.

2.2 Production pathways and process bottlenecks

2.2.1 Natural biomass feedstocks. The widespread use of natural biomass feedstocks for the production of NCCs involves pyrolysis as a key thermochemical conversion pathway. Some nitrogen-rich biomass feedstocks (such as microalgae, tobacco stems, *etc.*) can directly produce bio-oil with high nitrogen content through pyrolysis, with the absolute nitrogen content sometimes reaching as high as 10 wt% or even higher,[32] as shown in Scheme 1. The main NCCs in bio-oil include amines, amides, NHCs, and nitriles. By pyrolyzing protein-rich microalgae, the main NCCs in the bio-oil are hexadecylamide (selectivity of 42.86%), hexadecyl nitrile (selectivity of 17.87%), and indole (selectivity of 26.44%). The NCCs in bio-oil mainly originate from the cleavage of various amino acids in the microalgae proteins and intermediate reactions, including deamination and Maillard reactions.[33,34] Alternatively, direct pyrolysis of wastewater sludge rich in various amino acids can also be used. In this process, lysine in the sludge undergoes intramolecular cyclization to form lactams, which then undergo two successive cleavage steps with gradual dehydrogenation, resulting in stable NHCs. Tryptophan, after decarboxylation, deamination, dehydrogenation, and denitrification, gradually transforms into stable indole.[35] The NHCs in the bio-oil obtained by directly pyrolyzing nitrogen-rich biomass primarily include five-membered compounds (such as pyrrole, indole, pyrazole, and imidazole), six-membered compounds (such as pyridine, piperidine, pyrimidine, pyrazine, and quinoline), and piperazine derivatives. Nitrogen-rich biomass exhibits different chemical and physical characteristics during pyrolysis. This process involves complex chemical reaction steps, including amino acid cleavage, peptide bond rupture, oxidation reactions, and molecular rearrangement. However, it is important to note that endogenous nitrogen exists in various forms during the conversion process, making precise control over nitrogen migration and conversion for the target product more complex. Moreover, most biomass in nature, when used as raw material for direct pyrolysis, typically produces bio-oil that is rich in oxygenated functional groups such as aldehydes, ketones, and furan derivatives. In order to achieve the large-scale formation of NHCs, it is necessary to introduce exogenous nitrogen during the pyrolysis process, such as solid nitrogen sources or gaseous nitrogen sources, to co-pyrolyze and produce NHCs.

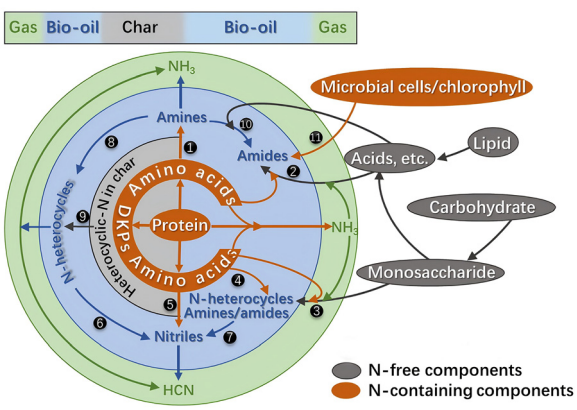

Scheme 1 Main nitrogen transformation pathways.[32]

Biomass nitrogen-rich co-pyrolysis is one of the most widely used methods for producing NHCs from raw biomass. Co-pyrolysis technology involves the simultaneous pyrolysis of biomass with an exogenous nitrogen carrier (such as urea, chitosan, chitin, ammonia gas, *etc.*), which can significantly increase the yield of NHCs. Ma *et al.*[36] investigated the nitrogen doping characteristics and nitrogen-rich pyrolysis product distribution of Moso bamboo at different pyrolysis temperatures by introducing an external gaseous nitrogen source, NH_3. They found that at 300 °C, the nitrogen content of Moso bamboo significantly increased from 0.03% to 7.59%. The relative content of NHCs in the bio-oil showed an increasing trend with the rise in pyrolysis temperature. Li *et al.*[37] studied the effects of different nitrogen sources (formamide, urea, melamine, and dicyandiamide) and impregnation concentrations on the nitrogen-rich co-pyrolysis products of biomass feedstock. The results showed that at a 5% impregnation concentration, formamide significantly increased the selectivity of NCCs, with a selectivity of 65.60%. The selectivity of pyrrole reached 27.41%, primarily due to the disruption of crystalline cellulose and the increase in furan selectivity. Additionally, the nitrogen source impregnation pretreatment of the feedstock reduced the activation energy of its pyrolysis reaction (from 23.71 to 12.35–20.82 kJ mol^{-1}). Bi *et al.*[5] co-pyrolyzed the three biomass components—cellulose, hemicellulose, and lignin—with urea and found that during the nitrogen-rich co-pyrolysis process, there were strong interactions between cellulose, hemicellulose, and lignin, as well as between these components and urea. Additionally, by tracking the evolution of intermediate chemical structures and the formation of final products, they identified that the aldehyde, ketone, and furan compounds, which are abundant in bio-oil as primary pyrolysis products of biomass, serve as precursors for NHCs, thus enabling nitrogen-rich transformation.

To better produce and enrich specific target NHCs in bio-oil, catalytic ammonia conversion has been widely studied as an effective approach. Yao and Zhang *et al.*[21,38] have emphasized that the unique structure and acidic sites of the HZSM-5 zeolite catalyst significantly enhance the rate of biomass conversion into NHCs in the thermocatalytic ammonia conversion

(TCC-A) process. Compared to MCM-41, USY, Hβ, HY, and γ-Al_2O_3, HZSM-5 achieved the highest total yields of bio-oil and acetonitrile, which were approximately 1.51–3.85 times and 2.14–3.68 times higher than those of the other supports, respectively. The TCC-A process is currently a key method for efficiently converting biomass into NHCs based on nitrogen-rich pyrolysis. However, there is limited research on catalyst selection and optimization, particularly the catalyst's resistance to coke deposition and its regeneration capacity. The study of the mechanism of its role in the conversion of NHCs is not yet comprehensive and warrants systematic research and exploration.

Other production methods also include hydrothermal treatment, gasification and syngas synthesis, as well as combined catalysis and multi-reaction processes. Hydrothermal reactions, conducted under subcritical or supercritical water conditions, can gently convert natural biomass (such as lignocellulose and algae) into platform compounds (*e.g.*, FF and HMF). These platform compounds can subsequently be used in the TCC-A process to produce NHCs.[39] Gasification and syngas synthesis, under high-temperature conditions, generate syngas (a mixture of CO and H_2), which can further react with ammonia or amines to produce NHCs. Optimization of gasification conditions—such as temperature, pressure, and gas flow rate—can enhance the reaction efficiency between ammonia and syngas, significantly increasing the yields of pyridine and indole compounds.[40,41] Combined catalysis and multi-step reaction production tend to favor a multi-pathway design optimization approach. Due to the inherent complexity of natural biomass, the direct conversion efficiency to target NHCs is relatively low. Therefore, optimizing multi-step reaction processes in conjunction with different catalytic systems has gradually emerged as an effective strategy.

2.2.2 Aldehyde and ketone platform compounds. Aldehyde and ketone platform compounds, owing to their abundant functional groups and high chemical reactivity, have become ideal intermediates for the production of NHCs. Although current industrial production still relies heavily on aldehydes and ketones derived from fossil-based feedstocks, the associated drawbacks are increasingly apparent. As a result, growing attention has been directed toward the value-added catalytic conversion of biomass-derived aldehydes and ketones, particularly focusing on the multifunctionality and broad applicability of catalysts to optimize and achieve efficient production pathways. Rational catalyst selection and reaction condition optimization not only enhance the yield of target NHCs but also offer a novel perspective for sustainable chemical production.

The most widely reported production strategy still relies on the excellent hydrogenation activity of noble metal catalysts to achieve high-yield and high-selectivity reductive amination of aldehydes and ketones, enabling the targeted synthesis of NHCs, as illustrated in Fig. 2. Representative catalysts include Ru-,[14] Pt-,[42] Rh-,[29] and Ni-[43] based catalysts.[42] Yang *et al.*[31] investigated the selective primary amination of alcohols, aldehydes, and ketones with ammonia, focusing on catalyst design

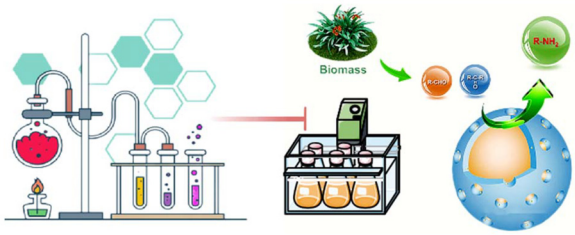

Fig. 2 High-selective reductive amination of aldehydes and ketones with noble metal catalysts.

and preparation strategies. These included the physical form of the catalyst, its acidity, and surface electronic density, aiming to enhance the heterogeneous catalytic performance for selective primary amine synthesis from alcohols, aldehydes, and ketones. Xu *et al.*[44] reported a yolk–shell structured Zr-assisted Ni-based catalyst. This catalyst showed high activity and strong stability in the reductive amination of various biomass-derived aldehydes and ketones. Under mild conditions (70 °C and 1 MPa H_2), the yield of FAM reached 99%. Other aldehydes and ketones were also efficiently converted to primary amines, with yields typically above 90%. Chen *et al.*[45] developed a N-quaternized pyridoxal catalyst, which exhibited high activity and stereoselectivity in the asymmetric Mannich reaction of biomass-derived carbonyl compounds. Liu *et al.*[46] developed a novel single-atom catalyst (Pd_1/BNC) using a supramolecular-controlled pyrolysis strategy. This catalyst efficiently converts biomass-derived aldehydes/ketones into a range of amine compounds, including primary, secondary, and tertiary amines. Throughout the integrated pyrolysis process, biomass-derived aldehydes/ketones undergo reduction amination *via* the Pd_1/BNC catalyst, with steps such as distillation, oxidative depolymerization, hydrolysis, and dehydration, ultimately producing amines with a low carbon footprint. Wang *et al.*[47] explored the direct catalytic nitration of aromatic amines and NHCs using N_2. This approach benefits from the *in situ* generation of Li_3N and its coordination catalysts, with Li acting as the reductant in the entire process. It is important to note that most biomass-derived aldehyde/ketone systems contain multiple functional groups. Considering the selective conversion of a specific functional group by a single precious metal catalyst is not entirely applicable to the production of NHCs from biomass.

2.3 Purification and application challenges in complex systems

The products of biomass-derived pyrolysis and catalytic conversion are typically composed of various functionalized compounds, including aldehydes, ketones, phenols, and other nitrogen-containing derivatives. Due to the complex chemical properties and diverse composition of primary pyrolysis products, the separation and purification of target chemicals becomes a bottleneck for industrial applications. This is particularly true for NHCs, which share similar chemical properties with by-products, making traditional separation

methods such as distillation and extraction inefficient. In recent years, the integration of heterogeneous catalytic systems with advanced separation technologies has become a key approach to addressing this challenge. For example, adsorption separation techniques, combined with the selective adsorption properties of porous materials, can effectively separate NHCs from other by-products. On the other hand, membrane separation technology, due to its efficiency and low energy consumption, has gradually gained attention. By designing functionalized membrane materials with specific pore sizes and surface chemical properties, separation efficiency can be significantly enhanced. Moreover, novel separation technologies based on molecular recognition and complexation effects offer potential solutions for the fine separation of complex systems. Specifically, focusing on biomass-derived aldehyde/ketone platform compounds, thermodynamic and kinetic analysis of the key reaction pathways can help minimize non-selective hydrogenation and reduce other competing reactions during the process. This approach, which maximizes control over by-product formation, will aid in the directed enrichment and conversion of aldehydes and ketones into NHCs. In conclusion, efficiently extracting high-value NHCs from complex systems requires breakthroughs in reaction pathway design, catalyst optimization, and separation technology development. These studies will not only promote the application of biomass-derived products in chemical production but also lay the foundation for achieving green and sustainable chemical manufacturing.

3. Biomass-derived carbonyls catalytic conversion potential to NHCs

3.1 Multifunctional reaction characteristics

Biomass-derived aldehydes and ketones exhibit multifunctional reactivity during chemical transformation processes. They are widely recognized as key platform compounds in the chemical industry, primarily due to their diverse chemical reactivities and high conversion flexibility. Owing to the high reactivity of their carbonyl groups and structural diversity, these compounds serve as ideal intermediates for the production of various high-value chemicals, making them increasingly prominent in both experimental research and industrial applications. Certainly, this is not limited to NHCs. A thorough understanding of the multifunctional reactivity of these platform compounds is crucial for optimizing the production processes of a wide range of chemicals.

3.1.1 Aldehydes. Taking FF and HMF as examples (Fig. 3), their rich functional groups endow them with distinct electronic properties and steric hindrance, which in turn determine their reactivity. Under the catalysis of metals such as Pd or Ru, these compounds can be selectively converted into products such as furfuryl alcohol and tetrahydrofurfuryl alcohol, which are widely used in the pharmaceutical and fragrance industries. In addition, HMF can be catalytically hydrogenated to produce 2,5-bis(hydroxymethyl)tetrahydrofuran (BHMTF), a

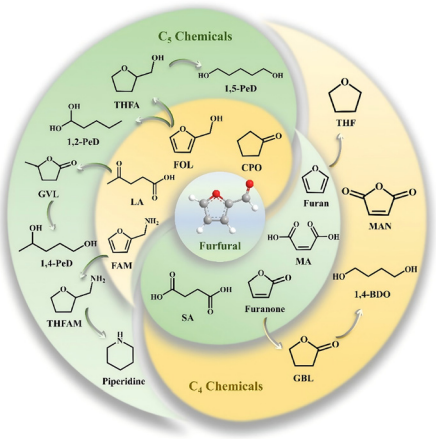

Fig. 3 Premium conversion applications of biomass-derived platform compound FF.[13]

potential bio-based monomer for polymer production. FF, primarily derived from hemicellulose, is a typical α,β-unsaturated aldehyde with various structural forms. The furan ring and aldehyde group in its molecular structure exhibit high reactivity in a wide range of chemical transformations. Zhang *et al.*[48] synthesized a well-dispersed Cu/MgO–La_2O_3 catalyst with bifunctional active sites *via* a simple impregnation method. The use of transition metals also addresses the limitations associated with noble metal catalysts, such as limited availability and high cost. A furfural-to-furfuryl alcohol conversion yield of 99.9% was achieved through selective hydrogenation. This high efficiency is attributed to the thermodynamically favorable C=O bond reduction and the low activation energy provided by the La–Cu bifunctional catalytic system. Also, the strong adsorption of FF facilitated the enhancement of the hydrogenation reaction. The two active sites provided by La and Cu enable simultaneous activation of hydrogen and FF. Moreover, the weak adsorption of the resulting furfuryl alcohol suppresses side reactions, thereby contributing to the excellent catalytic selectivity. FF, due to its strong reactivity, can undergo highly selective conversion in multi-component catalytic systems. FF and acetophenone can also be selectively hydrogenated over Pd nanocluster catalysts supported on sulfur-doped mesoporous carbon spheres. This process simultaneously produces tetrahydrofurfuryl alcohol and 1-phenylethanol, achieving a conversion rate of 99% and a selectivity of over 90%.[49] 1-Phenylethanol is also an important intermediate for the synthesis of analgesics, anti-inflammatory drugs, and fragrances.[50] To effectively utilize the chemical properties of FF platform compounds, researchers have continuously developed low-cost catalysts with high catalytic applicability. By exploiting the enhanced hydrogenation characteristics and reaction rates of FF through alloying, a CoNi alloy catalyst (*x*Co*y*Ni/C) was prepared *via* a one-step pyrolysis of a metal–organic framework (MOF), which is used for the hydrogenation of FF to produce tetrahydrofurfuryl alcohol. The formation of the CoNi alloy leads to a reconfiguration of the electronic

structure on the metal surface, which in turn affects the adsorption of functional groups on FF and furfuryl alcohol. The bimetallic CoNi alloy catalyst exhibits significantly more favorable adsorption of reactants and a higher hydrogenation rate, reflecting the kinetic enhancement arising from modified surface electronic density and reduced energy barriers for hydrogen activation.[51] HMF, a product of cellulose degradation, has its hydroxymethyl and aldehyde group structures that can be selectively converted into various chemicals under acidic or transition metal catalytic conditions,[52,53] such as 5-methylfurfural, 5-methylfurfuryl alcohol, 2,5-dimethylfuran, and 2,5-bis(hydroxymethyl)furan (BHMF).[54–56] Su *et al.*[57] first used heteropolyacid to promote the modification of a lignin-MOF-derived bimetallic catalyst, Ni_3Co-MOF-LS@HSiW, to improve its surface physicochemical properties. This modification enabled the high-selectivity conversion of HMF to 5-hydroxymethylfurfuryl alcohol. The *in situ* hydrogenation/deoxygenation of HMF was carried out on Ni_3Co-MOF-LS@HSiW, achieving a 100% conversion rate and a selectivity of up to 86.5%. Cai *et al.*[58] ingeniously developed nanofibers and porous carbon microspheres from chitin biomass polysaccharides, and encapsulated Fe–Ni bimetallic nanoparticles to form a novel catalytic nano-reactor (Fe–Ni/NPCMs). The Fe–Ni bimetallic nanoparticles were uniformly dispersed on the carbon nanofiber surface of Fe–Ni/NPCMs, providing abundant catalytic sites and excellent catalytic performance. Importantly, this reactor successfully achieved the high-selectivity hydrogenation of HMF to either BHMF or BHMTF. By simply adjusting the reaction conditions, Fe–Ni/NPCMs enabled the hydrogenation of HMF with high yields of 93.6% or 94.9% to BHMF or BHMTF, respectively. The differential activation barriers associated with hydrogenating the aldehyde and hydroxymethyl groups are effectively modulated by the electronic structure and dispersion of the Fe–Ni active sites. This provides a new platform for developing novel catalysts for the selective conversion of aldehyde and ketone platform compounds.

3.1.2 Ketones. Ketones, as representative platform compounds in condensation reactions, can generate various hydroxy ketones or unsaturated ketones through aldol condensation, providing important raw materials for fine chemicals. FF and acetone, as active representatives of aldehyde and ketone platform compounds,[59] are commonly used in typical aldol condensation reaction studies. The aldol condensation of aldehydes and ketones is a fundamental reaction in organic synthesis for forming C–C bonds (Scheme 2).[60] The aldol condensation of FF and acetone produces 4-(2-furanyl)-3-buten-2-one and 1,5-bis(2-furanyl)-1,4-pentadiene-3-one. This step is thermodynamically driven by the formation of conjugated enone structures, while the selectivity toward mono-condensation products requires kinetic control through catalyst acidity and spatial configuration. These aldol condensation products have been utilized for the preparation of functional polymers.[61] The condensation products can be further hydrogenated for use in biofuels.[62] To selectively control the aldol condensation pathway and suppress side reactions, efforts are

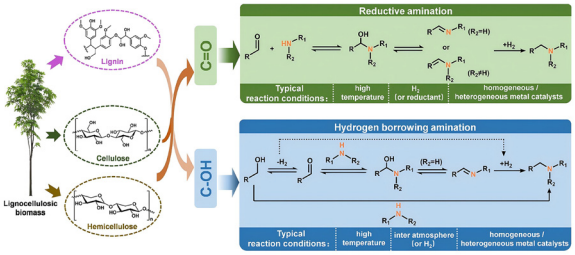

Scheme 2 The primary pathways for thermocatalytic amination of biomass-based compounds.[12]

focused on achieving high selectivity for the target products. More research has been concentrated on the development of efficient catalytic systems for the conversion of aldehydes and ketones. Deng *et al.*[63] aimed to control the aldol condensation of FF and acetone while suppressing dehydration to obtain β-hydroxy ketones. They found that the intrinsically inert boron nitride (BN), when calcined at high temperatures in air, could catalyze the aldol condensation of biomass-derived FF and acetone, yielding the highly selective hydrated product, 4-(furan-2-yl)-4-hydroxybutan-2-one. Additionally, two types of oxygen-substituted nitrogen defect sites on the air-calcined BN were identified, and their catalytic performance was successfully correlated with both dehydrated and non-dehydrated aldol condensation reactions. In catalytic systems with multifunctional acidic sites, the aldol condensation of FF and acetone can be achieved in a one-pot sequential process, followed by hydrogenation and deoxygenation to obtain alcohol-based target products. Medium-chain length alcohol compounds can be produced from FF and acetone through a series of reactions, including aldol condensation, hydrogenation, and hydrolysis.[64] A broader application of biomass-derived aldehydes and ketones in aldol condensation is the production of aviation fuel from biomass-derived aldehydes and ketones using a bifunctional catalyst, Ni/HZSM-5. In the Ni/HZSM-5 bifunctional catalyst, Brønsted acid sites are more effective than Lewis acid sites for the aldol condensation of aldehydes and ketones. The balance between the aldol condensation and hydrogenation active sites enhances the yield of alkanes to 62.91%.[65]

In addition to the typical reactions of certain aldehyde and ketone platform compounds, their ability to participate in oxidation reactions and the cyclization potential of carbonyl compounds have also gained significant attention. Taking FF as an example, under the influence of transition metal catalysts, it can be oxidized to furoic acid or further converted into furoic acid methyl ester, demonstrating its important role as a precursor for carbon-based platform chemicals. Similarly, the oxidation of FF can produce furoic acid, which is an important monomer for the preparation of corrosion-resistant polymer materials. For instance, using gold nanoparticles to catalyze the oxidation and esterification of FF to furoic acid methyl ester, the Au/γ-Al_2O_3-2 catalyst achieves a conversion rate of 99.6% and a selectivity of 99.5%.[66] FF can also undergo photo-

catalytic oxidation, where the photo-generated charge carriers of K-C_3N_4/UiO-66-NH_2 facilitate the photocatalytic oxidation of FF to furoic acid. The FF conversion rate reaches 89.3%, with a corresponding furoic acid yield of 79.8%.[67] In the field of energy utilization, traditional chemical oxidation methods for converting FF and other compounds into corresponding acids using molecular oxygen typically require high pressure to increase the solubility of oxygen in the aqueous phase, while electrochemical oxidation methods require the input of external electrical energy. To control energy consumption, Ouyang *et al.* developed a liquid-flow fuel cell system to achieve the oxidation of FF at the anode for the production of furoic acid and the co-production of hydrogen gas.[68] The cyclization reactions of carbonyl compounds typically involve reactions between biomass-derived molecules and ammonia or amines, catalytically forming C–N bonds. For example, the furan ring structure of FF can undergo a Diels–Alder reaction to generate various nitrogen-containing aromatic compounds. From a mechanistic perspective, the multifunctional reactivity of biomass-derived carbonyl compounds is governed by both thermodynamic and kinetic factors. Imine formation from aldehydes or ketones and ammonia is typically exergonic and thermodynamically controlled, while subsequent cyclization or hydrogenation steps often face higher activation barriers and rely on catalytic acceleration. In aldol condensation, C–C bond formation is thermodynamically favorable, but dehydration and polymerization are kinetically competitive, leading to side products. Similarly, the hydrogenation of furanic aldehydes such as FF and HMF involves parallel pathways influenced by reaction temperature, hydrogen pressure, and catalyst surface properties. In the field of NHCs production, biomass and its derived aldehyde and ketone platform compounds are particularly prominent. Their sustainability as precursors for the production of NHCs aligns with global development trends.[12]

In summary, aldehyde and ketone platform compounds, due to their multifunctional reactive characteristics, can participate in a wide range of chemical reactions, providing diverse conversion pathways for the chemical industry. These properties have allowed them to demonstrate significant potential in the fields of green chemistry, fine chemicals, and materials science.

3.2 Reactivity and NHCs precursor potential

Based on the multifunctional reactivity of the aforementioned platform compounds, aldehydes and ketones, with their highly reactive carbonyl group and flexible molecular structure, serve as key precursors for NHCs. Their chemical reactivity, particularly in ammoniation, condensation, and cyclization reactions, is central to their value, offering important pathways for the synthesis of NHCs. Typical aldehyde and ketone platform compounds, such as FF, can undergo nucleophilic addition with ammonia due to the synergistic effect of the furan ring and the aldehyde group, forming imine intermediates. These intermediates then undergo cyclization and dehydration reactions to yield pyridine derivatives. HMF, due to its hydroxymethyl and aldehyde groups, exhibits excellent condensation and cyclization potential, enabling the formation of pyrrole derivatives under acidic or metal-catalyzed conditions. Similarly, simple aldehyde and ketone compounds like acetone and formaldehyde, when reacted with ammonia, efficiently generate NHCs, highlighting their unique value in efficient transformation.

Typically, NHCs such as pyrrole, pyridine, and indole can be directly produced from furan *via* thermal catalytic conversion and zeolite-ammonia transformation.[69] However, furan (*e.g.*, furan, 2-methylfuran) is not easily produced in large quantities from abundant biomass sources, such as cellulose or carbohydrates.[70–72] Furan is mainly produced industrially from FF *via* decarbonylation.[73] Therefore, FF, with its synergistic furan ring and aldehyde group and its highly functional molecular structure, has gradually become a key player in the production of NHCs. Yao *et al.*[20] studied the production of indole from FF, systematically investigating the effects of reaction temperature, catalyst, weight hourly space velocity (WHSV), and the molar ratio of NH_3 to FF on product distribution. Using HZSM-5 (Si/Al = 25) as the catalyst at 650 °C, with a WHSV of 1.0 h^{-1} and an ammonia-to-furfural molar ratio of 2, the maximum indole carbon yield of 20.79% was achieved. Under the catalysis of HZSM-5 zeolite, the density of acidic sites on the catalyst significantly influences the selectivity of indole-based products. The conversion pathway of FF to indole can be validated through experimental and quantum computational results. Specifically, FF first reacts with NH_3 to form furfural imine, which then undergoes cleavage to generate furan. The furan intermediate is subsequently converted into pyrrole, which finally transforms into indole. The high reactivity of FF in this sequence is attributed to its conjugated aldehyde group, which readily forms stabilized imine intermediates and facilitates subsequent electron rearrangement during ring closure. Additionally, different reaction conditions (such as temperature and NH_3 flow rate) play a significant role in regulating the final product distribution, particularly the reaction environment and catalyst stability. Studies have shown that higher NH_3 concentrations do not necessarily increase the yield of the target NHCs. On the contrary, the increase in indole yield from FF is due to the dilution of NH_3, which suppresses the side reaction pathway that generates 2-furancarbothioamide and forms coke. Compared to pure NH_3, the catalyst in the N_2-diluted NH_3 reaction environment is more stable, with lower levels of dealumination, structural damage, and acid site loss.[21] Song *et al.* developed a process combining chemical and biological methods to produce renewable pyrrole from biomass-derived FF. They prepared a Pd-coated catalyst, with ultra-small metal nanoparticles encapsulated in zeolite channels to form a core–shell structure. In the fixed-bed catalytic system of Pd@S-1 and H-beta zeolite, FF was converted into pyrrole in a one-step decarbonylation–amidation reaction. This was the first successful demonstration of one-step decarbonylation–amidation of FF to pyrrole in the presence of NH_3 and H_2.[19] Ren *et al.*[74] reported a direct and environmentally friendly method for producing 3-hydroxy-pyridine from biomass-derived FF using a RANEY® Fe catalyst in

water. RANEY® Fe demonstrated effective catalytic activation of the furfural aldehyde group and achieved a 3-hydroxy-pyridine yield of 18.2% at 120 °C, with ammonia as the nitrogen source. HMF is another aldehyde platform chemical with excellent properties, typically obtained through the dehydration of fructose.[75] HMF can undergo condensation and ammoniation reactions to form pyrrole compounds. Due to the presence of numerous reactive functional groups in its structure, the synergistic effect of its hydroxymethyl and aldehyde groups enables the generation of high-value NHCs under acidic or metal-catalyzed conditions.[76] In particular, the hydroxymethyl group can participate in intramolecular hydrogen bonding or dehydration, which enhances the electrophilicity of the adjacent carbonyl and promotes cyclization. Bartosz Wozniak *et al.*[25] efficiently synthesized biomass-derived *N*-substituted 2-hydroxymethyl-5-methylpyrrole from HMF in two steps. First, using an iridium complex catalyst, HMF was hydrogenated and ring-opened in a phosphate buffer solution (pH = 2.5) to obtain 1-hydroxyhexane-2,5-dione. Then, 1-hydroxyhexane-2,5-dione was reacted with various amines (including alkylamines, aromatic amines, and benzylamine) in ethanol at room temperature in a Paal–Knorr reaction, efficiently converting to *N*-substituted 2-hydroxymethyl-5-methylpyrrole without the need for a catalyst. This reaction method is mild, aligns with green chemistry principles, and the hydroxymethyl functional group in the product facilitates further functionalization. Additionally, it is important to note that the conversion of FF, including HMF, into NHCs is significantly influenced by the catalyst, which plays a decisive role in the final product distribution.[77] Whether it's the catalyst's pore size, metal loading, or acid site distribution, these factors can significantly enhance the yield of the target product by affecting the stability of intermediate formations.[13]

In addition to typical biomass-derived compounds, simple aldehyde and ketone compounds such as acetone and formaldehyde, due to their simplicity and high reactivity, have long been important intermediates in the synthesis of industrial chemicals (Scheme 3). In recent years, the catalytic reaction pathways of these compounds have gradually been expanded into the research field of biomass-derived platform chemicals.[78] Zhou *et al.*[79] used co-pyrolysis of cellulose and paraformaldehyde, combined with a commercial HZSM-5 zeolite catalyst under an ammonia atmosphere to produce pyridine derivatives. The catalyst had a Si/Al ratio of 83.3, and at 500 °C, pyridine, nitriles, and pyrrole were easily formed. The possible mechanism for pyridine production is that the pyrolysis intermediates of paraformaldehyde not only serve as precursors for pyridine formation but also act as alkylating agents, allowing for alkylation substitution to yield pyridine.[80] To synthesize NHCs, most methods involve condensation under acidic or basic catalysis. However, these processes are often non-selective and can lead to numerous side reactions, complicating the product. As a result, many researchers have focused on developing high-selectivity heterogeneous catalytic technologies. N. G. Grigorieva *et al.*[81] developed a layered H-Ymmm zeolite catalyst, which outperforms the H–Y zeolite catalyst in synthesizing pyridine-type chemicals. In the products formed by the reaction of formaldehyde and ammonia, H-Ymmm zeolite predominantly produced pyridine (up to 63%) and dimethylpyridine. The reaction of acetaldehyde with ammonia yielded 2-methyl-5-ethylpyridine with 87% selectivity, while the reaction of propionaldehyde with ammonia produced 2-ethyl-3,5-dimethylpyridine with 58% selectivity. N. G. Grigor'eva *et al.*[82] studied the cyclic condensation of formaldehyde and ammonia, propionaldehyde and ammonia, and the reaction of aniline with aldehydes and ketones to synthesize NHCs. They extensively explored the catalytic performance of amorphous mesoporous aluminosilicate ASM samples with different Si/Al molar ratios (40, 80, 160) in the synthesis of pyridine and other NHCs. The mesoporous aluminosilicate ASM sample with a Si/Al ratio of 40 exhibited the highest activity and selectivity in these reactions. Acetone can undergo ammonia condensation by forming an enol intermediate, reacting with ammonia to produce pyrrole derivatives. However, the activation of acetone often requires Lewis acid catalysts, as the enol intermediate is less stable and the ketone carbonyl is less reactive compared to aldehydes. Formaldehyde can react with ethylenediamine in a one-step process to generate imidazole derivatives with high yield, a process that requires high selectivity of the catalyst.[83]

The reactivity of biomass-derived carbonyl compounds toward NHCs is closely related to their electronic structure and functional groups. Aldehydes, being more electrophilic than ketones, more readily undergo nucleophilic addition with ammonia. α,β-Unsaturated carbonyls like FF benefit from conjugation, which stabilizes intermediates and facilitates cyclization. In contrast, saturated ketones often require stronger catalytic activation due to steric hindrance. Multifunctional carbonyls such as HMF or acetoacetic acid offer multiple transformation routes, but also lead to side reactions from competing active sites. Thus, electronic effects, steric factors, and catalyst interactions collectively determine reactivity and product selectivity.

Compared to traditional fossil resources, biomass-derived aldehyde and ketone platform compounds offer a green advantage. These compounds are renewable and environmentally friendly, which not only reduces the carbon footprint during production but also provides a raw material foundation for achieving a circular economy (Fig. 4). Under nitrogen-rich conditions, the co-pyrolysis of biomass generates aldehyde and

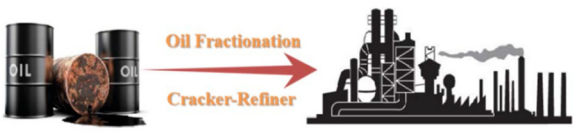

$$2C_2H_4O+CH_2O+NH_3 \rightarrow C_5H_5N+3H_2O+H_2$$

$$C_2H_4O+C_5H_5N \rightarrow C_6H_7N+CH_2O$$

$$2CH_2O+H_2 \rightarrow C_2H_4O+H_2O$$

Scheme 3 Industrial synthesis of NCCs from aldehydes and ketones.

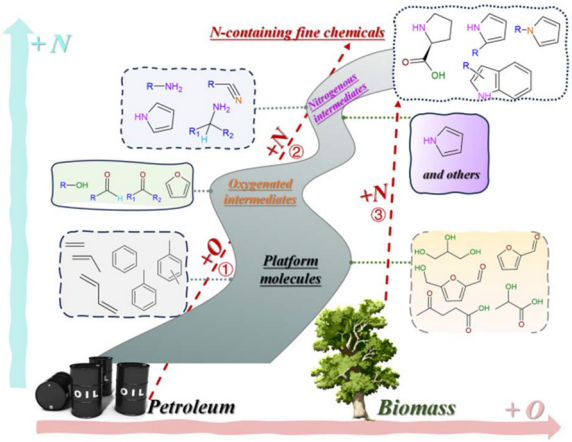

Fig. 4 Simplified routes to NCCs from petroleum and biomass resources. ① "+O": oxidation or dehydrogenation of petroleum hydrocarbons to oxygenates (Cu, Pd, acid catalysts, 200–350 °C); ② "+N": amination/cyclization of oxygenates to NCCs (NH_3, Ni, Ru, HZSM-5, 300–500 °C); ③ "+N": biomass undergoes direct N-rich pyrolysis to form NCCs in one step (urea or NH_3 co-feeding, 400–600 °C).

ketone platform compounds, which not only exhibit excellent chemical reactivity, providing high-quality precursors for the green production of NHCs, but also offer a practical model for studying the reaction competitiveness and selectivity of NHCs. Biomass-derived compounds provide valuable data support for the precise regulation of catalysts and theoretical modeling. Through the rational design of catalysts and the fine-tuning of reaction conditions, the selectivity toward target NHCs can be further improved, while minimizing the formation of by-products. Aldehyde- and ketone-based platform compounds, with their outstanding chemical reactivity and diverse reaction pathways, demonstrate significant value in the production of NHCs. In-depth investigation of the mechanisms of ammoniation and cyclization reactions of aldehyde- and ketone-based compounds, the development of efficient and green catalytic systems, and the integration of theoretical calculations with experimental studies to elucidate key reaction steps and side-reaction suppression mechanisms will provide essential support for the sustainable production of chemicals and the deeper understanding of their reaction pathways.

4. Mechanistic pathways for NHCs formation

4.1 Mechanistic analysis of multi-substrate reactions

The production of NCCs still heavily relies on fossil-based resources to date.[84,85] Developing green, simple, and efficient biomass-derived synthesis routes has become a common goal in both academia and industry. Lignocellulosic biomass, mainly composed of cellulose, hemicellulose, and lignin, can be effectively depolymerized through hydrolysis, enzymatic hydrolysis, pyrolysis, and other processes.[86,87] For instance, monosaccharides derived from the degradation of cellulose and hemicellulose can be further converted into FF and HMF,[88] while lignin can be transformed into a range of aromatic aldehydes and ketones.[89] These biomass-derived aldehydes and ketones, owing to their rich functional groups and highly tunable chemical reactivity, have been widely employed in the synthesis of NCCs, including but not limited to primary amines, NHCs, and *N*-substituted secondary and tertiary amines.[90] For example, cellulose and hemicellulose-derived compounds such as HMF, FF, cyclopentanone, and 2-pentanone, as well as lignin-derived compounds such as benzaldehyde, acetophenone, cyclohexanone, and cyclohexanecarboxaldehyde, can be effectively converted into primary amines under suitable conditions.[44,91] The reaction pathways for the production of NCCs typically involve key steps such as nucleophilic addition, condensation, cyclization, and dehydration. In particular, the transformation of aldehydes and ketones into NCCs often requires the selective conversion of C–O, C═O, or C═C bonds into C–N bonds. The reaction pathways include the reductive amination of R-CHO or R-C(O)-R′, borrowing hydrogen amination of R-OH, and hydroamination of C_nH_2 or C_nH_{2n-2} ($n \geq 2$).[92,93] However, it is worth noting that extensive experimental studies and theoretical analyses have revealed that the specific reaction mechanisms are significantly influenced by multiple factors, including substrate type, catalytic environment, and reaction conditions.

4.1.1 Aliphatic aldehydes and ketones. Aliphatic aldehydes and ketones (*e.g.*, formaldehyde, acetone, acetaldehyde, and propionaldehyde), due to their simple structures, readily undergo nucleophilic addition with ammonia or amines under catalytic conditions to form corresponding imine intermediates. These intermediates can then undergo intramolecular cyclization to yield five-membered heterocycles such as pyrroles and imidazoles, or six-membered nitrogen-containing rings such as pyridines. For instance, the reaction of formaldehyde with ammonia in an ethanol system, catalyzed by zeolites or amorphous mesoporous aluminosilicates, can efficiently produce six-membered nitrogen heterocycles like pyridine and its derivatives.[94] The main products obtained include pyridine (**I**), 2-, 3-, and 4-methylpyridines (**II**), as well as dimethylpyridines (**III**), with 3-methylpyridine accounting for as much as 80% of the total product distribution.[82] The proposed reaction scheme and pathway are illustrated in Scheme 4. In this scheme, the reactants serve as the starting point of the transformation pathway, while the zeolite catalysts and amorphous aluminosilicates play a crucial role in directing the formation of the final products. The NHCs obtained over mesoporous aluminosilicates are predominantly methylpyridines, whereas the products synthesized using zeolite catalysts such as H-ZSM-5 and Pb-ZSM-5 are mainly pyridine. Notably, significant changes in the product distribution can also be observed when the alcohol solvent is varied, even with the same reactants. When *n*-propanol is used as the solvent, 3,5-dimethylpyridine (**IV**) becomes the main product, accompanied by moderate amounts of 3,4-dimethylpyridine (**V**) and 2-ethyl-3,5-dimethylpyridine (**VI**) in the product mixture. When the solvent is switched to *n*-butanol, 3,5-di-

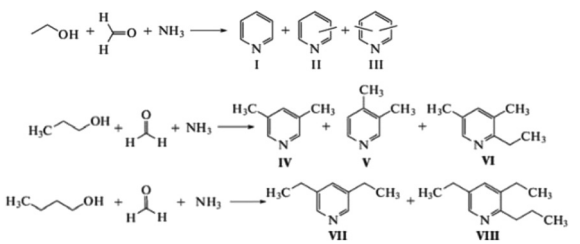

Scheme 4 Catalytic conversion of formaldehyde and ammonia to six-membered heterocycle pyridine and its derivatives.[82]

ethylpyridine (**VII**) is the predominant product, while 2-propyl-3,5-diethylpyridine (**VIII**) is formed as a by-product.[82] In the production of NCCs from formaldehyde and ammonia, six-membered nitrogen heterocycles such as pyridine and its derivatives are the main products. However, it is noteworthy that the production process is highly dependent on the type of alcohol solvent used and the nature of the catalyst employed.

In addition, several other compounds, such as acetaldehyde and propionaldehyde, serve as ideal feedstocks for the production of NCCs and do not necessarily rely on alcohol solvents in the reaction system. Currently, one of the most widely used approaches involves the reaction of acetaldehyde with ammonia in the presence of ammonium salts to produce methyl ethyl pyridine, achieving a yield of up to 60% with a selectivity of 88%. In this reaction pathway, the conversion rate of acetaldehyde reaches 69%, with 2-methylpyridine generated as a minor byproduct. The reaction of propionaldehyde with ammonia mainly yields 2-ethyl-3,5-dimethylpyridine. However, a variety of pyridine derivatives are also formed as byproducts, including pyridine, dimethylpyridine, and 4-ethyl-3,5-dimethylpyridine, among which the latter is identified as the major byproduct in the propionaldehyde–ammonia system. The conversion rate of propionaldehyde reaches 69.5% (Scheme 5).[82]

It is evident that aliphatic aldehydes and ketones, especially those with simple structures, remain the dominant feedstocks for the aldehyde/ketone-ammonia method in the synthesis of NCCs. However, these simple aldehydes and ketones are typically derived from fossil-based platform compounds. Despite the well-known issues associated with fossil-derived aldehyde–ammonia synthesis, such as pollutant emissions and harsh reaction conditions, it still represents the mainstream industrial demand. This is mainly because biomass-derived aldehyde/ketone platform chemicals have yet to be fully adapted for large-scale industrial production.[3] Although the production

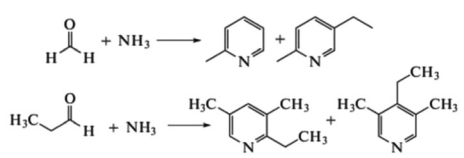

Scheme 5 Catalytic amination of other simple aldehydes to NHCs.[82]

of high value-added NCCs *via* pyrolysis of biomass and its simple aldehyde/ketone derivatives holds great significance, current research reviews indicate that biomass-derived simple aldehydes and ketones still lag behind fossil-based counterparts, particularly in terms of industrial application.[7] Nevertheless, ongoing efforts by researchers continue to advance the development and application of biomass-based NCCs. For simple aliphatic aldehydes and ketones, 2,5-hexanedione is a versatile organic intermediate with significant value in chemical and material industries due to its high boiling point and excellent solubility.[95] As it is derived from typical biomass feedstock such as cellulose, it is often used as a high-value biomass platform molecule for the production of value-added chemicals.[96,97] 2,5-Hexanedione, characterized by its simple structure and suitable bifunctional carbonyl groups, can be converted *via* reductive amination to synthesize *N*-substituted tetrahydropyrroles.[98] However, direct reductive amination of 2,5-hexanedione presents challenges regarding the hydrogenation anti-poisoning ability of metal catalysts. Hua *et al.*[99] developed functional catalysts by loading Ru nanoparticles onto HAP and montmorillonite for the conversion of biomass-derived 2,5-hexanedione to *N*-substituted tetrahydropyrroles. The catalytic transformation pathway is shown in Scheme 6a. Under the catalyst's action, 2,5-hexanedione underwent direct reductive amination at lower temperatures and shorter reaction times, achieving a 99% conversion rate and producing the target *N*-substituted tetrahydropyrrole. Typically, directly using amino-containing reactants simplifies the reaction steps, eliminating the need for external nitrogen sources or high-pressure conditions. As shown in Scheme 6b, amino acids and aldehydes undergo decarboxylation and dipolar ion formation, followed by cyclization to form substituted pyridines without the need for various metal catalysts.[100] Additionally, fusion with aniline or substituted aniline can synthesize NHCs, as shown in Scheme 6c.

4.1.2 Aromatic aldehydes and ketones. In the synthesis of NCCs, the conversion of aliphatic aldehydes and ketones still largely relies on fossil resources, whereas the research on aromatic aldehydes and ketones is more focused on biomass resources. This difference is influenced not only by the maturity of existing industrial pathways but also closely related to

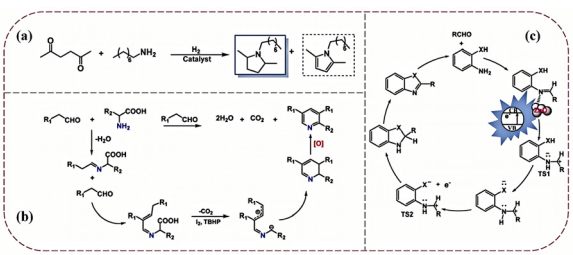

Scheme 6 (a) Conversion of biomass-derived 2,5-hexanedione into *N*-substituted tetrahydropyrroles using Ru-based catalysts; (b) decarboxylative oxidation and cyclization of amino acids and aldehydes to form pyridine; (c) synthesis of NHCs from aniline and its derivatives with aldehydes.[99–101]

the molecular structural characteristics and cracking mechanisms of the two types of compounds. Aliphatic aldehydes and ketones, such as formaldehyde, acetaldehyde, and acetone, have simple structures and are typically derived from the oxidative degradation of small molecular units. In catalytic oxidation or partial oxidation processes of fossil resources, alkanes, alkenes, and their derivatives can efficiently generate these compounds, making them the primary method for obtaining aliphatic aldehydes and ketones in the current chemical industry. As a result, traditional aldehyde–ketone-ammonia synthesis techniques have long relied on fossil resources, establishing a stable industrial production system. However, the main components of biomass (cellulose, hemicellulose, and lignin) tend to generate aromatic compounds with conjugated systems or carbonyl-conjugated structures, such as FF and vanillin, during pyrolysis or hydrolysis. This has shifted the focus of aromatic aldehydes and ketones research more towards biomass conversion, making them a key platform molecule for the development of renewable NCCs in recent years. Before discussing the conversion of aromatic aldehydes and ketones, it is important to mention the significance of the furan structure in the process of biomass-derived NCCs, despite not having aldehyde or ketone characteristics. As a typical five-membered oxygen-containing heterocycle, furan possesses a highly active conjugated system, which enables it to generate various NHCs through reactions such as amination and cyclization during catalytic conversion. Biomass-derived furan is often used in the production of NHCs, such as indole, due to its structural characteristics. Many reactions begin with furan as a starting material to generate 1,4-diketones (A: Yuriev reaction, B: Butin reaction, C: Achmatowicz reaction).[102] Subsequently, the furan-2-(2-aminobenzyl) undergoes ring-opening rearrangement upon oxidation with *meta*-chloroperoxybenzoic acid at 0 °C, followed by oxidation with 10% trifluoroacetic acid at room temperature, as shown in Scheme 7. In this process, the yield of indole exceeds 90%. Additionally, using HZSM-5 as a catalyst, the catalytic ammoniation of furan to indole (33.04% yield) is promoted by a 25% N_2-diluted NH_3 mixture, effectively suppressing side reactions in this mixed reaction system.[21]

FF, as one of the primary furan derivatives, retains the conjugated system of the furan ring and possesses an active aldehyde group, making it more advantageous in the synthesis of NCCs. In the synthesis of the nitrogen-containing heterocyclic chemical indole, experimental analysis and theoretical calculations suggest that the Diels–Alder mechanism is not favorable for indole formation. Whether starting with furan or FF, a ring-opening mechanism is more conducive to indole formation in the system,[20] as shown in Scheme 8a. The widespread demand for NCCs in daily life, industrial applications, and the pharmaceutical industry continues to drive the development of efficient synthesis processes for renewable NCCs, with biomass-derived FF serving as a key substrate. In production applications, primary NCCs are mainly FAM, and through further ring-opening rearrangement of FAM, piperidine can also be formed. FF can also directly undergo decarbonylation and ring-opening rearrangement to form pyrrole (Scheme 8b).[103] Typically, the catalytic reductive amination process of FF follows basic reaction stages. First, the aldehyde functional group undergoes nucleophilic interaction with ammonia to form an imine intermediate. The imine intermediate is then hydrogenated catalytically to produce the primary amine product, FAM. Chatterjee *et al.*[104] provided experimental evidence supporting the detailed mechanism of amine formation through an imine-mediated pathway. Although imine species were not directly observed during the analysis and monitoring process, the spectral identification of Schiff base-type compounds in the reaction system indirectly suggested the involvement of imine intermediates in the reaction process (Scheme 9a). Parallel studies by Nishimura *et al.*,[105] although detecting similar transient species, proposed a different mechanistic interpretation. Their findings suggested that FF preferentially undergoes nucleophilic addition with ammonia to form furanamide derivatives, which

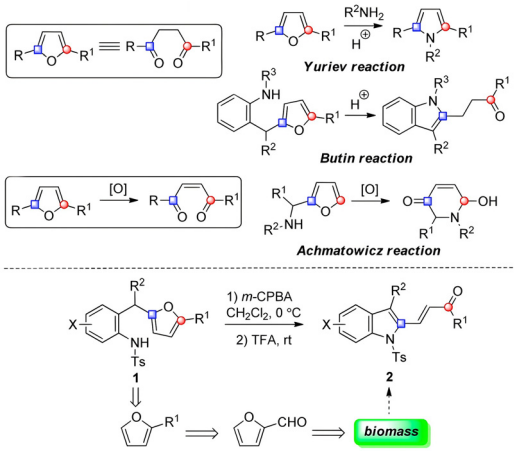

Scheme 7 Catalytic conversions of furan to NHCs.[102]

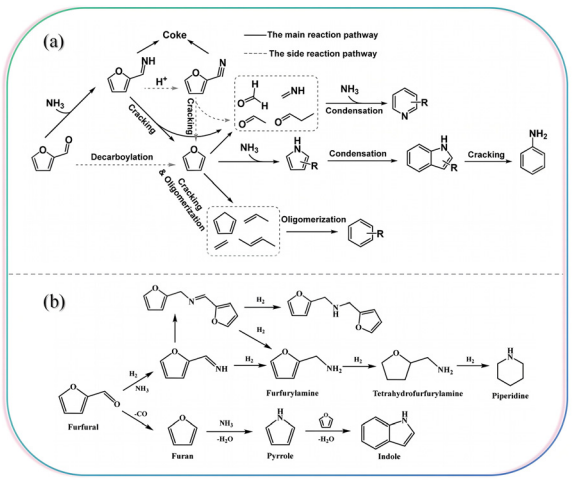

Scheme 8 Possible reaction pathways for the conversion of FF to various NHCs.[20,103]

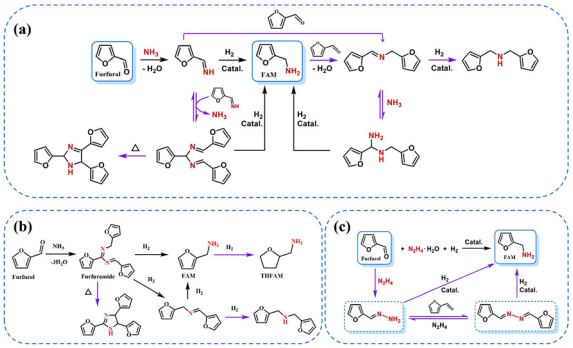

Scheme 9 Catalytic reductive amination reaction networks of FF.[7,104,105]

are then catalytically converted through hydrogenolysis of these intermediates, ultimately leading to the formation of FAM (Scheme 9b). However, due to the inherent reactivity between primary amines and carbonyl compounds, the formation of secondary amines is inevitable during the reaction, and primary amines may also appear as byproducts. Additionally, the selectivity of FAM is affected by side reactions, particularly the occurrence of hydrogenation and aldol condensation reactions. To reduce the hydrogenation byproducts of FF and suppress condensation reactions, Zou *et al.*[7] employed a reductive amination strategy using hydrazine hydrate ($N_2H_4{\cdot}H_2O$) as the nitrogen source. Their study found that under these conditions, FF is first converted into (2-furanylmethylene)hydrazine and 1,2-bis(2-furanylmethylene)hydrazine. Subsequently, under a hydrogen atmosphere, hydrogenolysis occurs, ultimately producing FAM. The rapid formation of the hydrazone intermediate and its moderate reactivity play a key role in enhancing the selectivity of FAM, making the reaction pathway more controllable (Scheme 9c).

4.1.3 Multifunctional aldehydes and ketones. In the research of biomass-derived aldehydes and ketones, simple aldehydes and ketones (such as formaldehyde, acetaldehyde, acetone, *etc.*) are widely used in the synthesis of NCCs due to their well-defined structure and controllable reactions. Aromatic aldehydes and ketones (such as FF, vanillin, *etc.*), due to the chemical stability of their conjugated systems, play an important role in biomass catalytic conversion. However, compared to these two types of compounds, multifunctional aldehydes and ketones better reflect the characteristics of primary biomass derivatives. Biomass is a highly complex, multi-component polymer system. During its pyrolysis or catalytic conversion, derivatives with multiple functional groups are often generated, such as acetylacetone, ethyl formate, and acetoacetic acid. These molecules not only retain the aldehyde and ketone structures but may also contain functional groups such as carboxyl, hydroxyl, and ester groups. As a result, multifunctional aldehydes and ketones can provide a wider range of reaction pathways in the synthesis of NCCs, including nucleophilic addition, condensation, decarboxylation, and cyclization, among other conversion methods.

It is important to note that, corresponding to the diverse reactivity of multifunctional aldehydes and ketones, is the complexity of the product composition. Due to the multiple chemical reaction sites in these compounds, various possible intermediates and byproducts are often formed in the reaction system, which limits the selectivity of the final target compound. This high reactivity and the resulting uncertainty in synthetic pathways have made research on the directed catalytic conversion of multifunctional aldehydes and ketones relatively limited. Lin *et al.*[106] used acetylacetone as the catalytic precursor to synthesize a novel bifunctional acetylacetone-based molybdenum catalyst (Ov-Mo-acac) with oxygen vacancies and acid sites. This catalyst was employed to catalyze the retro-aldol reaction of *N*-acetylglucosamine (NAG), which then underwent condensation and dehydration with acetylacetone, ultimately generating furan and pyrrole compounds. As shown in Scheme 10a, the reaction mechanism for synthesizing furan and pyrrole derivatives from NAG and acetylacetone involves cleavage and dehydration reactions. Initially, the bond dissociation and cleavage produce *N*-acetylaminoacetaldehyde (NAMD) and erythrose, which undergo dehydration–condensation with acetylacetone *in situ*. Subsequently, the reaction gradually progresses to form pyrrole and furan derivatives. Wang *et al.*[107] developed a highly efficient multifunctional catalyst by immobilizing CoNi alloy nanoparticles on nitrogen-doped porous carbon for the reductive amination of acetoacetic acid to nitrogen-substituted pyrrolidone. In this transformation, the key process involves the catalytic reductive amination of acetoacetic acid with benzylamine. The efficiency of this conversion is attributed to the synergistic catalytic effect of the catalyst, enabling the continuous and stable reductive amination of acetoacetic acid and amines (Scheme 10b). Additionally, some studies have explored the hydrogenation

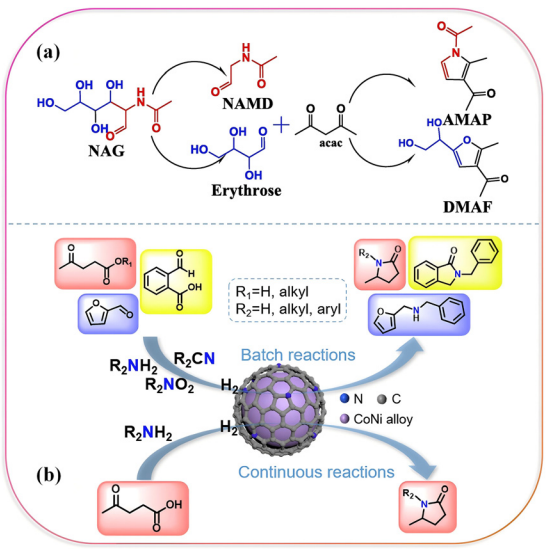

Scheme 10 (a) Catalytic retro-aldol reaction of NAG to form furan and pyrrole derivatives; (b) continuous and stable reductive amination of acetoacetic acid with amines.[106,107]

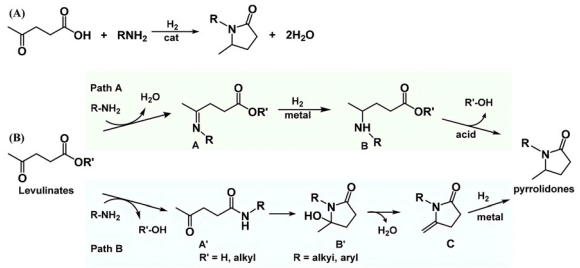

Scheme 11 (A) Traditional method for synthesizing pyrrolidone from acetoacetic acid and primary amines; (B) two potential pathways for pyrrolidone formation mechanisms.[108,109]

and reductive amination reactions of acetoacetic acid in heterogeneous systems.[108,109] As shown in Scheme 11, the reductive amination reaction of acetoacetic acid with cyclohexylamine proceeds primarily *via* two pathways. First, the carbonyl carbon reacts with the primary amine to form a Schiff base (**A**), which is then reduced to a secondary amine (**B**). Subsequently, intramolecular cyclization occurs, leading to the formation of pyrrolidone. The alternative pathway involves the reaction of the primary amine with the carboxyl group to form an amide compound (**A′**). This is followed by intramolecular cyclization to produce an intermediate (**B′**), which then undergoes a dehydration reaction to form an enamine (**C**). Finally, hydrogenation occurs, leading to the formation of pyrrolidone. Indeed, whether it is aliphatic aldehydes and ketones, aromatic aldehydes and ketones, or multifunctional aldehydes and ketones, catalytic amination or hydrogenation is the most crucial step in the preparation of NCCs. Therefore, highly efficient catalysts that play various catalytic roles in these reactions are essential. Various multifunctional catalysts and their catalytic mechanisms are continuously being studied and developed for more effective utilization.

4.2 Thermodynamic, kinetic characteristics, and side reaction control

4.2.1 Thermodynamic and kinetic competition in main reactions. In the reaction process, the formation of the target product is influenced not only by the structure of the reactants but also by thermodynamic and kinetic control. In the reaction system of FF and ammonia, the formation of imines is typically a thermodynamically controlled step, while the subsequent cyclization is a kinetically driven process.[110] It is evident that the free energy change during imine formation is relatively small, but the energy barrier of the cyclization step is significantly affected by the catalyst. In the widely used industrial reactions of aliphatic aldehydes and ketones, the cyclization reactions are often kinetically limited and require catalyst activation to lower the energy barrier. For example, the enol intermediate of acetone, due to its high energy state, typically requires additional Lewis acid sites to catalyze its stable formation of the pyrrole ring structure. ZnO can significantly lower the energy barrier of the acetone ammoniation reaction, greatly enhancing pyrrole selectivity.[111,112] The conjugated system of aromatic aldehydes and ketones provides a lower free energy state. As a result, cyclization reactions of aromatic aldehydes and ketones can occur under milder conditions, offering more flexibility in catalyst selection.

In the nitrogen-rich pyrolysis or nitrogen doping process of biomass and its derivatives, the thermodynamic control steps primarily involve the primary thermal degradation of biomass feedstocks, as well as the pyrolytic polymerization of cellulose, hemicellulose, lignin, and degraded sugars. Meanwhile, various endogenous and exogenous nitrogen sources can be converted under thermodynamic control into various nitrogen-containing intermediates or radicals, including $-NH^*_2$, $-NH^*$, NH_3, and $R_1R_2C{=}NR_3$, among others.[16,32] The formation of these nitrogen-containing chemical species not only provides important nitrogen sources for subsequent reactions but also influences the distribution of the final target products. Particularly in the Maillard reaction system, NH_3, $-NH^*_2$, $-NH^*$, and imines are considered key reaction intermediates, frequently appearing in research and literature related to the production of NCCs.[5,113,114] The thermodynamic control steps primarily involve the generation and distribution of nitrogen precursor species during the biomass pyrolysis process. It is worth noting that although the formation of imines typically exhibits a small change in free energy ($\Delta G \approx -5.2$ kJ mol^{-1}),[115] the reaction rate of this process is limited by the activation entropy required for proton transfer. Therefore, the reaction paths in different systems still need to be further confirmed through Density Functional Theory (DFT) calculations. However, it is unquestionable that this process does not require kinetic driving. In contrast, the synthesis of target NCCs often involves kinetically controlled steps, typically including key reactions such as ammoniation, reduction, substitution, condensation, cyclization, dehydrogenation, and addition, which form C–C/C–N bonds.[116] During these processes, the generation of high-energy intermediates makes it difficult for the system to solely rely on thermodynamics to drive the reaction toward the target products. Additionally, in kinetically controlled transformations, if the catalytic effect is insufficient, side reactions often dominate, such as polymerization, cross-condensation, or excessive oxidation, leading to the generation of a significant amount of non-selective by-products. For example, in the furfural–ammonia system, the activation energy for the cyclization reaction is typically high (>50 kJ mol^{-1}).[117,118] If the reaction is driven solely by thermodynamics without the involvement of a catalyst, it is often limited by slow reaction rates and complex side reaction pathways. Metal oxide catalysts (*e.g.*, ZnO, ZrO_2) can effectively stabilize the transition state (TS) and lower the activation energy to around 30 kJ mol^{-1}, thereby enhancing the main reaction process and improving the selectivity of the target product to over 90%.[119,120]

In addition, the structure of different types of reactants plays a crucial role in determining the reaction kinetics. Aliphatic aldehydes and ketones (*e.g.*, acetone) typically involve enol intermediates that lie in high-energy states (TS energy barriers >60 kJ mol^{-1}), and therefore generally require Lewis

acid catalysts (such as Zn^{2+})[121] to stabilize the intermediates and facilitate the formation of nitrogen-containing five-membered heterocycles, such as pyrrole. Aromatic aldehydes and ketones (*e.g.*, benzaldehyde, FF) generally exhibit lower cyclization energy barriers (<40 kJ mol^{-1}) due to their conjugated systems, enabling cyclization reactions to occur under mild conditions.[122] Such reaction systems can accommodate a broader range of catalysts, including weakly acidic zeolites (*e.g.*, HZSM-5) and non-metal catalysts. This catalytic flexibility is one of the key reasons for the extensive research and numerous advancements in the production of NCCs from these substrates.[20,21,69]

4.2.2 Microkinetic modeling and pathway optimization. In the catalyst-driven conversion of NCCs under kinetically controlled conditions, insufficient catalytic efficiency often leads to the dominance of side reactions, resulting in the formation of by-products such as polymerization, cross-condensation, or over-oxidation, as discussed in the previous section. Therefore, the core of pathway optimization lies in the rational design and fine-tuning of catalysts to selectively steer the reaction pathway toward the desired product with improved selectivity and controllability. In practical studies, pathway optimization is essentially closely related to the selection and design of catalysts. By tuning the composition, structure, and properties of active sites, the catalytic efficiency can be enhanced and energy barriers reduced, thereby promoting the formation of desired products. It is worth noting that microkinetic modeling is primarily applied to heterogeneous catalytic reaction systems. Its core lies in constructing a detailed reaction mechanism model to describe the rate, energy barriers, and evolution of intermediates for each elementary step, thereby providing quantitative guidance for catalyst optimization and reaction process control.

In current research on microkinetic modeling of heterogeneous catalytic reaction systems, different modeling approaches are selected based on the scale of investigation, including atomic, mesoscopic, and macroscopic levels, as illustrated in Fig. 5. In practical applications, microkinetic modeling primarily focuses on transport processes and is employed to elucidate the conversion mechanisms of biomass, its derivatives, or model compounds.[123] The kinetic parameters obtained through microkinetic modeling applications help reveal the interactions between reactants and catalysts, and clarify their potential reaction pathways.[124] As a quantitative analytical tool for complex reaction systems, microkinetic modeling provides a detailed kinetic description of heterogeneous catalytic systems by analyzing elementary reaction steps, rather than using aggregate rate constants.[125] This model in catalytic reaction studies mainly covers three core stages: the adsorption process of reactants on the catalyst surface, the surface transformation reactions between adsorbed species, and the desorption behavior of products.[125] Notably, this framework also integrates the potential impact of mass transfer effects on the overall reaction kinetics. To implement microkinetic simulations, it is necessary to systematically obtain a multi-dimensional parameter set, which specifically includes: the pre-exponential factor of each elementary reaction, adsorption/desorption equilibrium coefficients, catalyst active site coverage distribution, and the activation energy barriers for each step.[125] Among these, surface adsorption-related parameters can be obtained through synchrotron radiation characterization techniques or DFT calculations, while reaction rate constants and energy barrier parameters need to be jointly determined through temperature-dependent kinetic experiments, combined with *in situ* characterization of catalysts and analysis of reaction components.[125] In attempting to obtain specific kinetic parameters for the production and conversion of NCCs, it is crucial to have a systematic theoretical framework for kinetic evaluation. A stepwise, layered approach not only ensures the theoretical rationality of the model parameters but also enables iterative optimization of the model through experimental data validation. The simplest and most fundamental model used in microkinetic modeling for analyzing and evaluating reaction processes is the power law kinetic model.[124] It is an empirical model commonly used in the study of heterogeneous catalytic reaction dynamics.[126] In the degradation process of organic compounds, zero-order or first-order reaction models are commonly used to describe their kinetic characteristics.[127,128] This method can generalize the basic kinetic properties of reactions, especially suitable for heterogeneous systems. If the reaction is assumed to be second-order, the description equation is:[124]

$$-r = kC_A^n C_B^m \quad (1)$$

In this equation, r is the reaction rate, C is the concentration of the specific reactant, and n and m correspond to the reaction orders of the specific reactants. However, the power-law equation has certain limitations. Its ability to fit experimental data is constrained by the measurement range, and it can only be used for kinetic analysis within specific parameter limits. It is worth noting, however, that it can be extended to more complex kinetic evaluations to explain effects such as heat transfer, mass transfer, and catalyst deactivation.

As described in most literature, the heterogeneous catalytic process begins with the adsorption of reactants onto the cata-

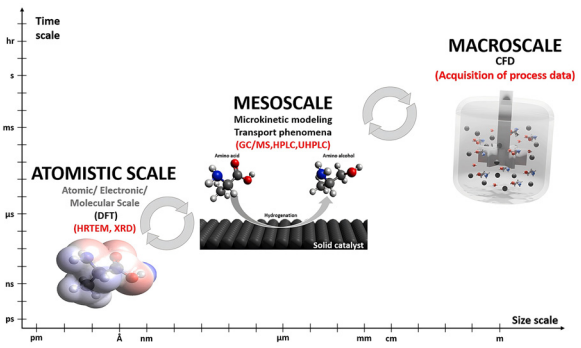

Fig. 5 Multiscale modeling approaches in the production of high-value NCCs.[116]

lyst surface, followed by the reaction and desorption processes. Over the course of extensive research and development, it is believed that after the adsorption of reactants, the conversion of the reactants into products can be primarily divided into two different mechanisms: the Langmuir–Hinshelwood mechanism (LH) and the Eley–Rideal mechanism (ER) (Fig. 6).[129] The LH involves the adsorption of reactants, diffusion to the active sites on the catalyst surface, the reaction at these active centers to form adsorbed products, and finally the desorption of the products from the catalyst surface (Fig. 6a).[130] This model assumes that the catalytic reaction primarily occurs on the catalyst surface. Both reactants A and B must adsorb onto the catalyst surface site #, where they react in the adsorbed state. Subsequently, product C desorbs and enters the gas phase. During this process, the adsorption rate is much faster than the surface reaction rate (*i.e.*, adsorption reaches equilibrium).[131] Additionally, the reaction rate is influenced by the coverage of adsorbed species on the catalyst surface and is positively correlated with their product. The reaction mechanism is described in the following form:[132]

$$1.\quad \# + \mathrm{A} = \#\mathrm{A} \tag{2}$$

$$2.\quad \# + \mathrm{B} = \#\mathrm{B} \tag{3}$$

$$3.\quad \#\mathrm{A} + \#\mathrm{B} \rightarrow 2\# + \mathrm{C} \tag{4}$$

$$\mathrm{A} + \mathrm{B} \rightarrow \mathrm{C} \tag{5}$$

The rate equation can be written as:

$$r = \frac{kc_{\mathrm{A}}RTc_{\mathrm{B}}RT}{\left(1 + K_{\mathrm{A}}c_{\mathrm{A}}RT + K_{\mathrm{B}}c_{\mathrm{B}}RT\right)^2} \tag{6}$$

$$P = cRT \tag{7}$$

where r is the reaction rate, c is the concentration, k is the reaction rate constant, K is the adsorption equilibrium constant, P is the partial pressure in the gas phase, R is the gas constant, and T is the temperature.

By substituting the gas phase partial pressure P into the rate expression, the simplified equation can be obtained as:

$$r = \frac{kP_{\mathrm{A}}P_{\mathrm{B}}}{\left(1 + K_{\mathrm{A}}P_{\mathrm{A}} + K_{\mathrm{B}}P_{\mathrm{B}}\right)^2} \tag{8}$$

In the reaction process of this mechanism, the adsorption rate is much faster than the surface reaction rate (*i.e.*, adsorption reaches equilibrium). Additionally, the reaction rate is influenced by the coverage of adsorbed species on the catalyst surface and is positively correlated with their product.

In the framework of the ER, there are different options for the adsorption behavior of reactants and products. It assumes that one reactant adsorbs onto the catalyst surface and transforms into an adsorbed state, which then reacts with another substance in the gas phase. The reaction product then desorbs.[133] In the ER pathway, one reactant adsorbs on the catalyst surface, while the other gas-phase reactant directly interacts with the adsorbed species, forming the product without the need for additional adsorption sites (Fig. 6b).[129] This reaction mechanism is described by the following form:

$$1.\quad \# + \mathrm{A} = \#\mathrm{A} \tag{9}$$

$$2.\quad \#\mathrm{A} + \mathrm{B}\langle - \rangle \#\mathrm{C} \tag{10}$$

$$3.\quad \#\mathrm{C} = \# + \mathrm{C} \tag{11}$$

$$\mathrm{A} + \mathrm{B}\langle - \rangle \mathrm{C} \tag{12}$$

The rate equation can be written as:

$$r = \frac{kK_{\mathrm{A}}(c_{\mathrm{A}}RT)(c_{\mathrm{B}}RT)}{1 + K_{\mathrm{A}}c_{\mathrm{A}}RT} \tag{13}$$

$$P = cRT \tag{14}$$

where r is the reaction rate, c is the concentration, k is the reaction rate constant, K is the adsorption equilibrium constant, P is the partial pressure in the gas phase, R is the gas constant, and T is the temperature.

By substituting the gas-phase pressure P into the rate equation, the simplified expression can be obtained:

$$r = \frac{kK_{\mathrm{A}}P_{\mathrm{A}}P_{\mathrm{B}}}{1 + K_{\mathrm{A}}P_{\mathrm{A}}} \tag{15}$$

The reaction rate in the ER increases linearly with the coverage of the adsorbed molecules, which is quite different from the LH. However, similar to the LH, the reaction rate increases with the coverage of the adsorbates until it reaches a peak, and then decreases close to zero at 100% coverage. This is because the pre-adsorbed species block the adsorption sites for other reactants.[129]

In the research process, to perform a more comprehensive microkinetic analysis, researchers continuously consider incorporating various scenarios and condition parameters, including catalyst saturation scenarios. Based on the LH and ER, one of the most classic and universal models in heterogeneous catalytic reaction kinetics is the Langmuir–Hinshelwood–Hougen–Watson (LHHW) model. This model assumes that the adsorption–desorption process quickly reaches equilibrium, and the adsorption and desorption rates of reactants on the catalyst surface are much faster than the surface reaction rate. Meanwhile, the surface reaction is the rate-controlling step in the entire process.

Additionally, the catalyst surface is assumed to be uniform, with identical adsorption site energies and no interactions

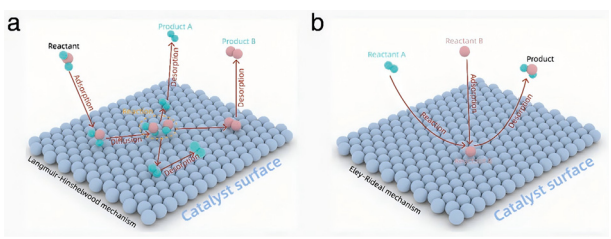

Fig. 6 Mechanisms of reactant conversion to products in multiphase catalytic processes: (a) LH; (b) ER.[129]

between sites. The rate equation of the LHHW model typically includes the following components:[116]

$$r = \frac{(\text{kinetic term}) \cdot (\text{thremodynamic driving term})}{(\text{adsorption or side blocking term})^n} \quad (16)$$

Here, r is the reaction rate; the kinetic term refers to the forward rate constant that determines the rate of reaction and is related to the rate constant k; the thermodynamic driving term represents the degree to which the overall reaction is close to thermodynamic equilibrium, or the balance between the product and reactant partial pressures; the adsorption or side blocking term accounts for the impact of species adsorption on the surface coverage; the parameter n refers to the number of surface active sites involved in the rate-determining reaction. Assuming a simple bimolecular reaction A + B → C, this reaction mechanism is described in the following form:

$$1.\quad A + \# \rightleftarrows A\# \quad (17)$$

$$2.\quad B + \# \rightleftarrows B\# \quad (18)$$

$$3.\quad A\# + B\# \rightarrow C\# + \# \quad (19)$$

$$4.\quad C\# \rightleftarrows C + \# \quad (20)$$

The rate equation can be written as:

$$r = \frac{kK_AK_BP_AP_B}{(1 + K_AP_A + K_BP_B + K_CP_C)^2} \quad (21)$$

where r is the reaction rate, c is the concentration, k is the reaction rate constant, K is the adsorption equilibrium constant, P is the partial pressure in the gas phase.

A review of the literature reveals that current research on microkinetic modeling is primarily focused on nitrogen transformation during the conversion of typical biomass components into NCCs. The reaction mechanisms are predominantly explored through DFT calculations. Yan *et al.*[134] constructed and simulated a cellulose/glutamic acid biomass polymer model using microkinetic modeling. By combining Reactive Force Field Molecular Dynamics (ReaxFF MD) with DFT calculations, they revealed the nitrogen migration and transformation mechanism during the formation of NCCs through pyrolysis and gasification of biomass. Chen *et al.*[135] produced pyrrole from cellulose under an ammonia atmosphere. Combining experimental results with DFT modeling, they proposed a novel ammonia-promoted pathway for pyrrole formation from cellulose. Xu *et al.*[136] investigated the kinetics and formation mechanism of NCCs from microwave pyrolysis of food waste. Using DFT calculations, they found that the process follows a first-order kinetic model. Carboxyl and carbonyl groups were more prone to cyclization with amino groups. It is worth noting that, current microscopic kinetic studies on the catalytic conversion of biomass and its aldehyde–ketone derivatives into NCCs still face significant challenges. When applying various microkinetic models to analyze these reactions, the precision of the kinetic description is limited by insufficient understanding of the key mechanistic steps in catalytic conversion. Particularly, the microscopic mechanisms of interfacial processes such as adsorption–reaction–desorption remain notably underexplored. In terms of the application and development of microkinetic modeling, the establishment of such models offers significant potential for integration with experimental studies. However, its practical application still faces several limitations. These include challenges in accurately determining kinetic parameters, especially for complex biomass-derived systems, as well as the high computational cost associated with modeling multistep reactions involving numerous intermediates and transition states. Therefore, future research should focus on developing multiscale simulation methods based on microkinetic modeling. By combining the advantages of power law kinetics, LH, ER, and the LHHW model, the establishment of an accurate microkinetic model can help predict the kinetic behavior of different catalytic systems. This provides theoretical guidance for optimizing catalyst design and enables effective control of reaction pathways. In addition, reducing the computational burden of modeling remains a critical priority. Not only can this reduce the blind spots in experimental screening and improve catalytic efficiency, but it will also provide crucial theoretical support for the efficient catalytic conversion of biomass and its derivatives into high-value NCCs in the future.

4.2.3 Side reaction mechanisms and suppression strategies. During catalytic reactions, the presence of various side reactions poses a significant challenge to optimizing reaction pathways and achieving high selectivity toward target products. In the catalytic conversion of biomass-derived aldehydes and ketones into NCCs, the main side reaction pathways include over-oxidation, cross-condensation, polymerization/carbonization, deamination/hydrolysis, and over-hydrogenation. These side reactions not only reduce the yield of desired products but can also lead to catalyst deactivation and accumulation of by-products. The over-oxidation pathway primarily occurs in the presence of oxidative catalysts (*e.g.*, CuO, MnO_2). During the catalytic amination process, the α-carbon of aromatic aldehydes (such as benzaldehyde and anisaldehyde) is prone to oxidation, ultimately forming carboxylic acids (RCOOH) or amides ($RCONH_2$).[31] This process is typically mediated by oxidative radicals (*e.g.*, $^{\bullet}OH$, O_2^-), with the formation of carboxylic acids exhibiting a Gibbs free energy change (ΔG) of approximately −30 kJ mol^{-1} at pH 7. However, due to the relatively high kinetic barrier (E_a > 80 kJ mol^{-1}), the reaction rate is strongly influenced by the electronic structure and oxidation potential of the catalyst surface.[137] Jiao *et al.* demonstrated that the use of a TiO_2/CuO type-II heterojunction photocatalyst can effectively modulate the band structure, reducing the valence band potential from +2.1 V to +1.5 V. This adjustment suppresses the formation of $^{\bullet}OH$, thereby preventing the further oxidation of aromatic aldehydes. Experimental results showed that this strategy increased the selectivity of aromatic aldehydes to over 99%.[137] In addition, the use of reductive supports (*e.g.*, TiO_{2-x}-supported Ni) can effectively suppress the oxidation state of active metals, thereby reducing the selectivity toward carboxylic acids from 40% to below 5% (XPS analysis confirmed that the proportion of Ni^0 exceeded 80%).[138]

The cross-condensation pathway primarily involves Aldol condensation reactions between aldehyde/ketone molecules. In multi-substrate systems, condensation typically occurs between the α-hydrogen of one molecule and the carbonyl group of another. For instance, during the co-reaction of FF and acetylpropionic acid, condensation byproducts can account for over 50%.[139] The key step in this process is the enolization of the α-carbonyl compound. In the study by Zhang *et al.*[140] on ethanol-to-butadiene conversion over MgO catalysts, it was found that the Meerwein–Ponndorf–Verley (MPV) reaction can induce the co-adsorption of acetaldehyde and crotonaldehyde, leading to the formation of highly activated enolized species, thereby promoting cross-condensation side reactions. DFT calculations indicated that the activation energy of this process is only 0.39 eV (approximately 37.6 kJ mol^{-1}). In addition, Gaggero *et al.*[141] reported that during intermolecular cross-linked benzoin-type condensation reactions, the use of azo salt precatalysts imparted high tunability to the condensation process. By modulating the catalyst, the proportion of condensation byproducts was reduced from over 50% to less than 10%, indicating that regulating adsorption sites significantly influences the selectivity of condensation side reactions. Furthermore, additional suppression strategies involve the utilization of spatial confinement effects. For example, modified microporous molecular sieves (pore size of 0.3 nm) can physically hinder the condensation of large molecules, significantly enhancing the selectivity of target products in systems like cyclopentanone–furfural.[142] It is worth noting that under high temperatures or acidic conditions, uncontrolled condensation side reactions may further lead to polymerization and even carbonization. Typically, FF can undergo aldol condensation, dehydration, aromatization, and eventually graphitization under such conditions, thereby negatively impacting the selectivity toward target products. Therefore, precise control over catalyst properties and the reaction environment is essential to enhance the selectivity of desired products in condensation reaction systems.

The deamination/hydrolysis pathway mainly involves the instability of imine intermediates. In aqueous environments, imines (RCH═NH) are prone to hydrolyze back to aldehydes or ketones, leading to a reduction in the selectivity of the target products.[143,144] Yang *et al.*[145] found in their study on the synthesis of 2-hydroxy-3*H*-phenoxazin-3-ones that under alkaline conditions with a pH of 10, the yield of the target product was higher. However, when the pH exceeded 11, the hydrolysis rate of the imine intermediate increased significantly, leading to a 20% or more increase in the proportion of side products. EPR experiments further confirmed that the increase in free radical concentration accelerated the hydrolysis side reaction. Additionally, experimental data showed that under neutral conditions (pH = 6–8), the hydrolysis rate was the lowest (k_hydrolysis = 0.03 h^{-1}). However, under strong acid/strong base conditions, the proportion of side products exceeded 20%, indicating that pH has a significant impact on the hydrolysis side reaction. To address this, during the experiment, a dual-active-site cooperative catalysis strategy can be employed. For example, using Lewis acid (Zn^{2+}) to fix NH_3, while utilizing Brønsted acid (–SO_3H) to promote dehydration, significantly reduces the side reaction of imine hydrolysis.[146,147] In addition, strategies such as adjusting the energy band structure, optimizing the catalyst surface adsorption sites, controlling NO_x concentration and acid strength, as well as regulating pH and free radical concentration, can effectively suppress side reactions and thereby improve the selectivity and yield of the target products.

Although several side reaction pathways and corresponding catalytic inhibition strategies have been described for converting biomass-derived aldehydes and ketones into target products, many uncertainties remain. These uncertainties arise from various factors within the reaction system. For example, the reductive amination of FF to FAM involves a complex reaction network, not a simple one.[148] As shown in Scheme 12, although the synthesis route of FAM (**2a**) appears to only require the condensation of FF (**1a**) and ammonia, the actual reaction system presents significant kinetic challenges. The high reactivity of the aldehyde group and the thermodynamic instability of the imine intermediate lead to complex competitive transformation pathways: firstly, direct reduction of the aldehyde group generates the undesired product furfuryl alcohol (**6a**). Secondly, the imine intermediate (**7a**) may undergo trimerization to form NHCs (**3a**). More complexly, secondary condensation reactions can occur between the target product FAM (**2a**) and the starting material or intermediates, generating more stable secondary imine Schiff base (**4a**), which can further be hydrogenated into secondary amine derivatives (**5a**). These side reaction pathways significantly reduce the selectivity of the main reaction, presenting a significant challenge for optimizing reaction conditions. While various catalytic inhibition strategies have been developed to improve the selectivity of the target product, the complexity of the reaction system makes it difficult to completely avoid side reactions. Future research should focus more on catalyst design, optimizing reaction conditions, and dynamically controlling reaction pathways. This will help achieve directed inhibition of side reactions and enhance the yield and atom economy of the target product.

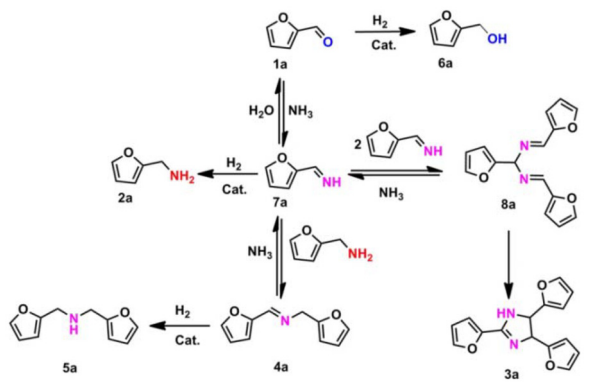

Scheme 12 FF reduction amination to FAM and potential side reactions.[148]

5. Catalyst roles in pathway modulation and selectivity optimisation

In the complex reaction network of the directed conversion of aldehyde/ketone substrates to NCCs, the catalyst plays a crucial role. It precisely controls key steps, such as C=O bond activation, NH_3/NH_2* species dissociation, and C–N bond coupling. This is achieved through fine-tuning the electronic structure of active sites, optimizing interfacial mass transfer dynamics, and applying multidimensional confinement effects. In metal-based catalyst systems, precious metals (such as Pt and Pd) exhibit irreplaceable advantages in the synthesis of high-value products like aromatic amines, owing to their excellent d-band electron regulation capabilities. However, they face challenges related to resource constraints and sustainability. Non-precious metals (such as Ni and Co) and their single-atom configurations (*e.g.*, Fe–N–C) have achieved significant optimization of the NH_3 dissociation energy barrier through coordination environment engineering and support synergistic effects, while reducing costs. As a key intermediary bridging coordination chemistry and molecular synthesis, metal catalyst systems have seen groundbreaking developments in both fundamental design and application in recent years,[11] as shown in Fig. 7. Especially, the synthesis of NCCs from biomass feedstocks and their derivatives mediated by metal catalyst systems has become one of the most typical and promising reactions,[11] as shown in Fig. 8. Non-metallic catalytic systems have opened up differentiated pathways. Molecular sieves regulate the protonation of intermediates through the dynamic balance of Brønsted/Lewis acidic sites. MOFs and nitrogen-doped carbon materials capture free radical species using editable pores and surface defect states. This inhibits excessive hydrogenation side reactions. Different catalytic systems offer atomic-level control and multidimensional selectivity in the amination/ammoniation reactions of aldehyde and ketone compounds. Their dynamic structure–activity relationships drive the precise synthesis of NCCs.

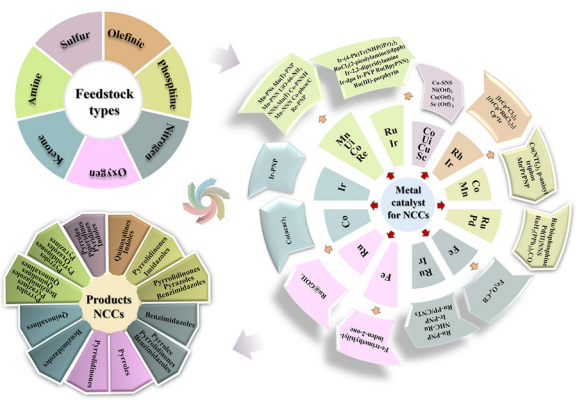

Fig. 7 Recent developments and applications of metal catalyst systems in the production of NCCs.

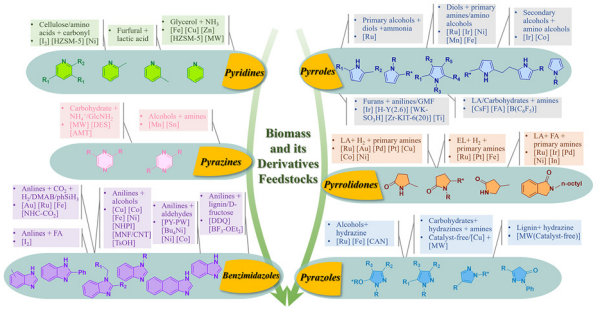

Fig. 8 Metal-catalyzed production of NHCs from biomass and its derivatives.

5.1 Metal-based catalysts

5.1.1 Noble metal catalysts. FF and HMF are widely available platform compounds for the high-selectivity amination of carbonyl compounds to produce NCCs (Table 1). In the catalytic amination system using Ru-based catalysts, early strategies focused on constructing $Ru^{II}(DMP)_2Cl_2$ complexes, which optimize the electronic structure through ligand engineering with spatial tension. The study employs a hydrogen pressure control strategy in an ethanol medium, utilizing the dual functional properties of primary/secondary amines to achieve the efficient nitrogen functionalization of the biomass platform molecule HMF.[149,150] Nishimura *et al.*[151] innovatively developed a Ru catalyst system supported on β-zeolite, achieving the directed reduction amination of HMF to produce 5-hydroxymethyl-2-furoylamide (HMFA) under NH_3/H_2 dual gas atmosphere control. The study found that the carrier acid–base regulation factor (SiO_2/Al_2O_3 ratio) affects catalytic performance through a dual mechanism: (a) it mediates the distribution of Ru nanoparticle size (ranging from 2.8 to 5.1 nm), and (b) it regulates the ratio of RuO_2/Ru_0 on the surface (confirmed by XPS). When the molar ratio was 150, the synergistically optimized metal dispersion (particle size of 3.1 nm) and oxidation state ratio (RuO_2 68%) led to a HMFA yield of 70%, revealing the structure–activity relationship between carrier properties, active site microenvironments, and catalytic performance. Chandra *et al.*[152] developed face-centered cubic ruthenium nanocrystals (2D-FCC-Ru-NPs), which exhibited outstanding performance in a methanol–ammonia control system (99% FAM selectivity, turnover frequency (TOF) = 1850 h^{-1}). The flat morphology induced interfacial electronic effects that weakened the metal d-band center, moderately reducing the electron-donating ability of Ru active sites. This precisely balanced the generation of imine intermediates and the hydrogenation rate. Comparative studies showed that the Ru-PVP/HAP composite catalyst (Ru-loaded HAP) used by Nishimura[105] achieved a 60% FAM yield under mild conditions (0.4 MPa H_2, 100 °C). However, its TOF (~320 h^{-1}) was significantly lower than that of the bare Ru NPs system. This difference arises from the steric hindrance effect of the PVP ligand layer and the HAP support's restriction on reactant diffusion dynamics. This also confirms the positive correlation

Table 1 Noble metal catalyst-mediated selective amination to produce NCCs

Type	Reactant	Catalyst	Nitrogen source and reductant	Temperature and time	Conversion	Ref.
Noble metal	HMF	Ru/BEA zeolite	$NH_3{\cdot}H_2O$, H_2 (0.6 MPa)	100 °C, 12 h	>70%	151
	FF	2D-FCC-Ru-NPs	NH_3 (8 mmol), H_2 (2 MPa)	90 °C, 2 h	99%	152
	FF	Ru-PVP/HAP	$NH_3{\cdot}H_2O$, H_2 (0.4 MPa)	100 °C, 2 h	>60%	105
	FF	Ru/BNC	$N_2H_4{\cdot}H_2O$, H_2 (2 MPa)	80 °C, 16 h	>99%	7
	FF	Ru/α-Al_2O_3	NH_3 (0.2 MPa), H_2 (2 MPa)	70 °C, 24 h	>60%	153
	FF	Ru/TiO_2	$NH_3{\cdot}H_2O$, H_2 (2 MPa)	120 °C, 2 h	>99%	154
	FF	Rh/Al_2O_3	NH_3, H_2 (2 MPa)	80 °C, 2 h	>90%	104
	FF	Pd/MoO_{3-x}	NH_3, H_2 (2 MPa)	80 °C, 4 h	>84%	155
	FF	Rh/Al_2O_3	NH_3, H_2 (2 MPa)	80 °C, 2 h	>91%	104
	Benzaldehyde	Pt/CoFe-LDH	NH_3, H_2 (2 MPa)	80 °C, 15 h	>95%	156

between metal exposure and catalytic efficiency. Zou *et al.*[7] designed a Ru-loaded boron–nitrogen co-doped carbon catalyst (Ru/BNC) that constructs a dual-active interface through frustrated Lewis acid–base pairs (FLPs). The FLPs promote the dissociation of hydrazine to supply nitrogen, while the Ru sites optimize the hydrogenation pathway. This electronic synergistic effect enables over 99% FAM selectivity for FF within 16 h under mild conditions (80 °C, 2 MPa H_2). The key mechanism lies in the FLPs-Ru interface, which accelerates the formation of hydrazone intermediates and inhibits excessive hydrogenation. Wang *et al.*[153] investigated the catalytic activity and selectivity of various active metals in the FF reduction amination reaction. They found that Ru-based catalysts exhibited the highest catalytic activity compared to other metal-based catalysts. The 1 wt% Ru/α-Al_2O_3 catalyst achieved a FAM yield of 61.9% after 24 h of reaction under the conditions of methanol, 0.2 MPa NH_3, 2 MPa H_2, and 70 °C.

In addition to Ru-based catalysts, noble metal catalysts such as Pd, Rh, and Pt also exhibit excellent catalytic performance in the reduction amination of carbonyl compounds. Studies have shown that the activity of palladium-based catalysts is closely related to their nanostructure and the metal–support interaction. Wang *et al.*[155] developed a Pd/MoO_{3-x} catalyst, optimizing the synergistic effect between Pd nanoparticles and the MoO_{3-x} support by adjusting the preparation temperature. Under 80 °C and 2 MPa H_2 for 4 h, the catalyst achieved an 84% FAM yield. Mechanistic analysis showed that the low-valent Mo species in the support not only act as Lewis acid sites to activate the aldehyde group but also regulate the electronic state of Pd through strong metal–support interactions, thereby promoting the amination process. In the HMF conversion system, a Pd/C catalyst with a particle size of 2.7 nm achieves a 94% HMFA yield in the presence of an ammonia source, owing to the exposure of high-activity unsaturated Pd sites. Its performance advantage stems from the synergistic regulation of crystal face effects and size effects.[157] For Rh-based catalysts, the Rh/Al_2O_3 system exhibits 91.5% FAM selectivity in the reduction amination of FF at 80 °C for 2 h. Further studies show that by optimizing hydrogen pressure, the hydrogenolysis pathway of the Schiff base intermediate can be controlled. This increases product selectivity to 85.5% and effectively inhibits the formation of secondary amine byproducts and cyclohydrogenation reactions.[104] In addition, in the Pt-based catalytic system (Pt/CoFe-LDH), Pt nanoparticles exhibit unique electronic structure regulation properties through strong electronic interactions with the CoFe layered double hydroxide (LDH) support.[156] As shown in the Fig. 9, the electronic migration from the support to the Pt active center significantly enhances the electron density of Pt, enabling excellent adsorption and activation of NH_3 and NH_4^+ in an ammonia-rich environment. Further *in situ* characterization revealed that the dynamically restructured Pt interface precisely controlled the orientation of reaction intermediates by introducing steric hindrance effects, effectively blocking side reaction pathways such as excessive alkylation. This interface engineering strategy led to a remarkable 95% selectivity for primary amine products, highlighting the synergistic control of electronic and geometric structures in Pt catalysts during reductive amination reactions.[156] These studies reveal the universal structure–activity relationship in precious metal catalysts for reductive amination reactions.

5.1.2 Non-noble metal catalysts. The cost limitations and resource scarcity of precious metal catalysts have driven the continuous development of non-precious metal catalytic systems for the aminative/aminolytic reactions of aldehyde and ketone compounds. Compared to precious metals, non-precious metals (such as Ni, Co, Cu, *etc.*) offer advantages in terms of cost-effectiveness and abundance. However, their early applications were often constrained by harsh reaction conditions and byproduct selectivity issues. With the emergence of strategies such as active site electronic structure regulation and support interface engineering, the reaction activity

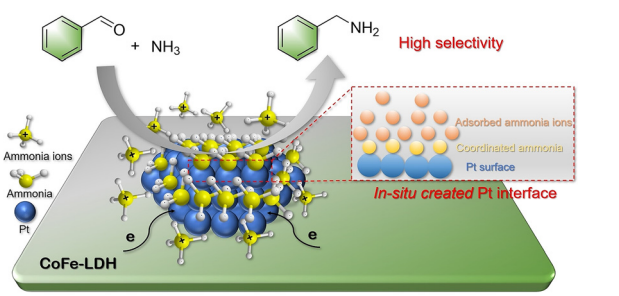

Fig. 9 *In situ* reconstruction of Pt interface and its coordination with ammonia.[156]

and selectivity of non-precious metal catalysts have been significantly enhanced.

For non-precious metals, particles of Ni, Co, Cu, and others supported on substrates serve as effective catalysts in the conversion of biomass-derived carbonyl compounds with NH_3 and H_2 into the corresponding amines and NCCs (Table 2). However, due to copper's relatively low hydrogenation activity and its widespread influence on carbonyl compound reductive amination, research on Cu-based catalysts in this reaction is relatively scarce. Most reported non-precious metal catalysts are primarily based on Ni and Co. Zhou *et al.*[158] used RANEY® Ni catalyst in tetrahydrofuran solvent to achieve 99.2% yield of FAM from FF by adjusting the NH_3/H_2 partial pressures (0.35/0.5 MPa) and reaction temperature (180 °C). DFT calculations showed that the similar adsorption energies of NH_3 and H_2 on the Ni surface could synergistically optimize the distribution of active sites, promoting the hydrogenation/dehydrogenation dynamic balance. Based on the active site regulation strategy, Song *et al.*[159] further designed a nitrogen-doped porous carbon-supported nickel catalyst (Ni/pNC). The Ni-NX active sites, where nitrogen interacts with Ni, significantly reduced the activation energy of the reaction, achieving a 92.3% yield of FAM at 60 °C and 3 MPa H_2. To further expand the substrate applicability, Yang *et al.*[162] developed a Ni/SiO_2 catalyst that utilizes the strong Lewis acidity of the support to preferentially adsorb the aldehyde group. Under conditions of 0.8 MPa NH_3, 4 MPa H_2, and 90 °C, the catalyst achieved 98% selectivity for FAM. However, catalytic stability under low-temperature conditions remains a challenge. To address this issue, Hu *et al.*[160] prepared the $Ni@C/Al_2O_3$-400 catalyst using a pyrolytic reduction strategy. The carbon protective layer effectively stabilized the Ni_0 active sites, maintaining >96% yield of HMFA under low-temperature conditions (30 °C, 2 MPa H_2). After six cycles, the activity only decreased by 7%. However, controlling side reactions in the complex reaction system still requires further breakthroughs. To address this, Liu *et al.*[161] designed a core–shell $Ni@SiO_2$-0.2 catalyst, where the SiO_2 shell with a pore size of 0.2 nm precisely controlled the reactant diffusion path through spatial confinement effects. This allowed HMF and HMFA to diffuse toward the Ni active sites, preventing HMF hydrogenation and 2,5-bis(aminomethyl) furan (BAMF) self-coupling. As a result, both HMF conversion and BAMF selectivity reached 99%, with stable performance maintained over seven cycles. In addition to optimizing single catalysts, multi-component synergistic strategies demonstrated unique advantages. Wei *et al.*[170] found that the combination of RANEY Co and RANEY® Ni enhanced the HMF to BAMF conversion rate beyond the limits of single catalysts. The synergistic mechanism is attributed to Co preferentially catalyzing hydroxymethyl amination, while Ni promotes aldehyde reduction. This discovery provides new insights for designing multi-step reactions. Wang *et al.*[171] achieved the conversion of HMF to BAMF through a stepwise catalytic pathway. The reduction amination step, catalyzed by RANEY® Ni, was combined with acid hydrolysis. This resulted in a final yield of 45.7% (Scheme 13).

Co catalysts have gained significant attention due to their abundant resources and cost advantages, leading to systematic progress in the catalysis of amination/aminolysis of biomass platform molecules. Chandrashekhar *et al.*[166] prepared Co/SiO_2 catalysts by pyrolyzing Co–terephthalic acid–piperazine MOF/SiO_2 precursors at 800 °C. Under mild conditions (50 °C, 1 MPa H_2), the catalyst achieved 94% yield of HMFA in the reduction amination of HMF with $NH_3{\cdot}H_2O$. The key advantage of this system is its broad substrate applicability, achieving over 95% yield of target amine products when reacting with primary amines, secondary amines, and *N*-alkyl amines, providing a versatile platform for various amination reactions. Yogita *et al.*[169] further optimized catalyst stability by preparing nitrogen-doped carbon-confined Co nanoparticles (Co/NC-700) *via* pyrolysis of ZIF-67. Due to the Co–N coordination, the catalyst achieved over 99% FAM yield within 1 h at 120 °C and 2 MPa H_2. This breakthrough demonstrates the unique value of nitrogen-doped carbon supports in stabilizing active centers.

Table 2 Non-noble metal catalysts for amination of biomass-derived carbonyl compounds

Type	Reactant	Catalyst	Nitrogen source and reductant	Temperature and time	Conversion	Ref.
Non-noble metal	FF	$Ni/CaCO_3$	$NH_3{\cdot}H_2O$, Zn/H_2O	80 °C, 10 h	>91%	26
	FF	RANEY® Ni	NH_3 (0.35 MPa), H_2 (0.5 MPa)	180 °C, 2 h	>99%	158
	FF	Ni/pNC	NH_3 (0.4 MPa), H_2 (3 MPa)	60 °C, 6 h	>99%	159
	HMF	$Ni@C/Al_2O_3$-400	$NH_3{\cdot}H_2O$ (7 mmol), H_2 (2 MPa)	30 °C, 16 h	>96%	160
	HMF	$Ni@SiO_2$-0.2	$NH_3{\cdot}H_2O$, H_2 (2 MPa)	170 °C, 12 h	>99%	161
	FF	Ni/SiO_2	NH_3 (0.8 MPa), H_2 (2 MPa)	90 °C, 1.5 h	100%	162
	FF	Ni/Al_2O_3–$0.5LaO_x$	NH_3 (2 MPa), H_2 (2 MPa)	90 °C, 1.5 h	>99%	163
	FF	$Ni_2P@C$-700	*N*-Butylamine, H_2 (1.4 MPa)	170 °C, 2 h	100%	164
	FF	15 wt% Ni/α-Al_2O_3	NH_3 (0.2 MPa), H_2 (2 MPa)	70 °C, 24 h	100%	153
	FF	Ni/Al_2O_3	NH_3 (0.4 MPa), H_2 (3 MPa)	60 °C, 4 h	>99.9%	165
	HMF	Co-NPs@SiO_2	$NH_3{\cdot}H_2O$, H_2 (1 MPa)	50 °C, 16 h	>99%	166
	Benzaldehyde	Co_2P NRs	$NH_3{\cdot}H_2O$, H_2 (0.1–1 MPa)	25 °C, 48 h	>87%	167
	FF	RANEY Co	NH_3 (0.1 MPa), H_2 (1 MPa)	120 °C, 2 h	100%	168
	FF	15 wt% Co/α-Al_2O_3	NH_3 (0.2 MPa), H_2 (2 MPa)	50 °C, 24 h	100%	153
	FF	Co/SiO_2	NH_3, H_2 (5.1 MPa)	130 °C, 10 h	100%	42
	FF	Co/NC-700	$NH_3{\cdot}H_2O$, H_2 (2 MPa)	120 °C, 1 h	100%	169
	FF	Co@C-600-EtOH	$NH_3{\cdot}H_2O$, H_2 (2 MPa)	90 °C, 4 h	>99%	117

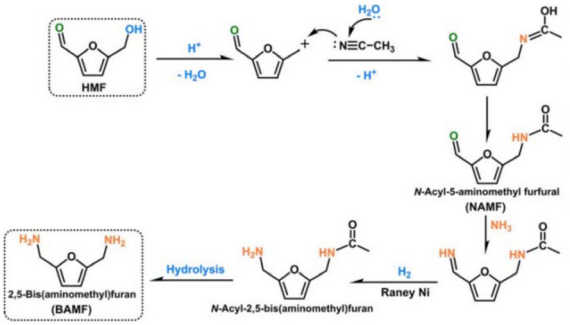

Scheme 13 Amination of HMF to BAMF conversion *via* distributed catalysis using RANEY® Ni.[171]

Zhuang *et al.*[117] approached from a green synthesis perspective and developed a multilayer graphene-encapsulated Co catalyst (Co@C-600-EtOH). Under conditions of 90 °C, 2 MPa H_2, and 7 mol NH_3 solution, the catalyst achieved over 99% FF conversion with 86.2% FAM selectivity. Through *in situ* infrared spectroscopy and DFT calculations, the researchers first revealed the bifunctional mechanism: the metal Co preferentially activates the C═O bond of FF to generate an imine intermediate, while the surface acidic sites promote hydrogenation of the imine to form the amine product (Fig. 10).[117] The catalyst's stable performance after 8 cycles highlights its potential for industrial applications. The contribution of Senthamarai *et al.*[172] lies in the amination of complex aldehyde and ketone molecules. They developed a MOF-derived Co-DABCO-TPA@C-800 catalyst featuring a coexistence of graphite-encapsulated Co nanoparticles and single-atom sites (Fig. 11). This catalyst enabled efficient amination of 39 aldehydes and ketones, including steroid derivatives and other pharmaceutical molecules, using gaseous NH_3. This work not only expands the scope of biomass conversion but also offers a novel tool for pharmaceutical molecule modification.

Inspired by the work of Senthamarai *et al.*,[172] Yuan and Elfinger *et al.*[173,174] designed a nitrogen-doped carbon-supported Co nanoparticle catalyst (Co@NC-800). The basic NH-functional groups on the support surface specifically enhanced the condensation step kinetics. Under mild conditions (50 °C, 10 bar H_2), the selectivity toward primary amines was 1.3 times higher than that achieved with noble metal catalysts, marking a significant breakthrough in developing non-noble metal catalysts for mild reaction conditions. Notably, the introduction of phosphorus alloying offers a new paradigm for tuning the electronic structure of Co-based catalysts. Single-crystalline Co_2P nanorods (Co_2P NRs) exhibit enhanced d-electron density at Co sites induced by phosphorus atoms (Fig. 12),[175] which lowers the H_2 dissociation energy to 26 kcal mol^{-1}. As a result, the catalyst enables highly selective conversion of HMF, FF, and other carbonyl compounds to the corresponding primary amines under low hydrogen pressures (0.1–1.0 MPa).[167] This study provides atomistic insights into the feasibility of replacing noble metal systems with non-noble metal catalysts.

Although Cu-based catalysts exhibit relatively lower overall activity compared to Co- and Ni-based systems, their unique advantages in specific reactions should not be overlooked. Calcination of Cu–Al LDH yields $CuAlO_x$ catalysts, which, owing to their strong Lewis acid sites, exhibit selective adsorption of aldehyde groups. In a flow reactor, they enable tandem amination–hydrogenation of HMF with aniline. It is now widely recognized that the catalytic amination or ammonolysis of carbonyl compounds such as aldehydes and ketones represent an efficient route for synthesizing high-value NCCs from ammonia. Noble metal catalysts have been extensively studied due to their high selectivity and catalytic efficiency. In contrast, non-noble metal catalysts are widely employed in practical applications owing to their abundance and cost-effectiveness.

5.1.3 Single-atom catalysts. Single-atom catalysts (SACs), featuring atomically dispersed active centers, unique electronic structures, and nearly 100% atomic utilization, have emerged as a promising class of catalysts for biomass-derived transformations in recent years. Compared to conventional metal nanoparticles or supported catalysts, SACs offer improved reaction selectivity and stability. This is achieved by precisely

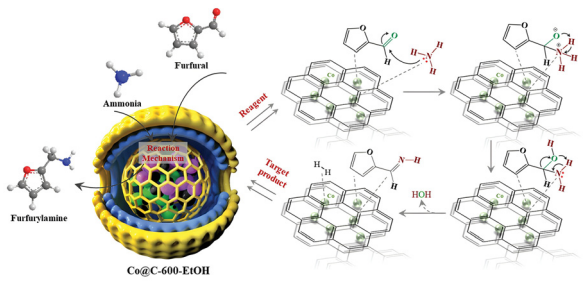

Fig. 10 Possible pathway for the reduction amination of FF with ammonia to FAM catalyzed by Co@C-600-EtOH.[117]

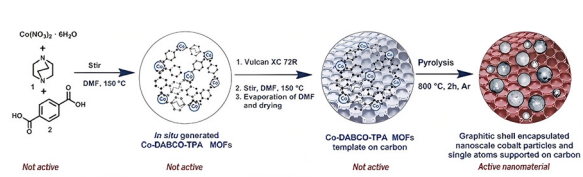

Fig. 11 MOF-derived Co-DABCO-TPA@C-800 catalyst with Co nanoparticles and single atoms.[172]

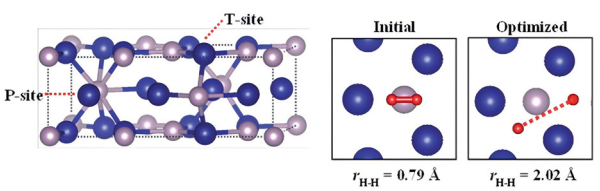

Fig. 12 Single-crystalline Co_2P nanorods (Co_2P NRs) structure simulation.[175]

tuning the local coordination environment of active sites, including the type, number, and spatial configuration of coordinating atoms. In addition, SACs help reduce the use of noble metals. In the catalytic conversion of aldehyde and ketone compounds to NCCs, SACs optimize the control of reaction intermediates. This enables selective activation of C=O bonds and suppression of side reaction pathways, providing an innovative solution for the green synthesis of high-value NCCs (Table 3).

One of the key strategies for optimizing the performance of SACs is the engineering design of the local coordination environment around the single-atom active sites. Liu *et al.*[46] prepared a palladium single-atom catalyst (Pd_1/BNC) supported on B and N co-doped carbon (BNC) *via* a supramolecular pyrolysis strategy (Fig. 13a). In this catalyst, Pd atoms are anchored on the support in a Pd–N_2–B coordination structure, forming highly polar metal N–B active sites. Experimental and theoretical studies revealed that the electron-deficient nature of B and the electron-rich nature of N synergistically induce a local electric field effect. This effect facilitates heterolytic cleavage of the hydrogen donor to generate active hydrogen species, which are then selectively transferred to the C=O bond to form imine intermediates. In the reductive amination of biomass-derived carbonyl compounds such as HMF and vanillin, Pd_1/BNC exhibits broad substrate applicability. It achieves primary amine yields of 90–96% and shows excellent tolerance toward sensitive functional groups such as hydroxyl and ether moieties. In addition, DFT calculations reveal a significant downshift in the d-band center of Pd in the Pd–N–B structure, which weakens the interaction with NH_3 and enhances the catalyst's ammonia tolerance. After seven reaction cycles, the catalyst maintains a 94% conversion rate and an 89% amine yield. Qi *et al.*[148] developed a N-doped C (NC) supported ruthenium single-atom catalyst (Ru_1/NC). By adjusting the pyrolysis temperature (700–1000 °C) and applying NH_3 post-treatment, the Ru–N_x coordination structure (x = 3–5) was precisely tuned (Fig. 13b). Among them, the Ru_1/NC-900-800NH_3 catalyst features Ru–N_3 as the dominant active site. The downshift of the d-band center enhances H_2 heterolytic dissociation while weakening the strong adsorption of NH_3. In

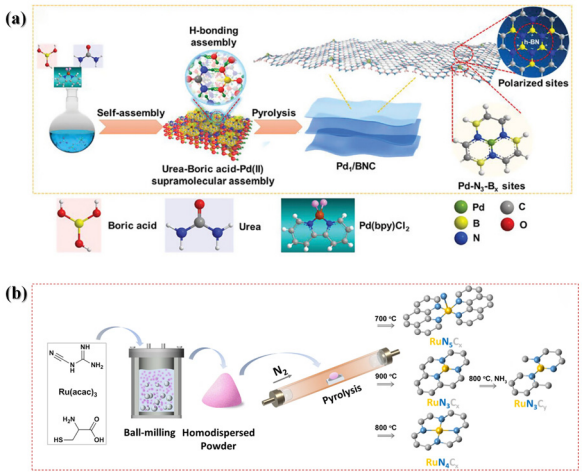

Fig. 13 (a) Schematic of Pd_1/BNC single-atom catalyst synthesis; (b) schematic of the synthesis of Ru_1/NC single-atom catalyst supported on nitrogen-doped carbon.[46,148]

the reductive amination of FF, the primary amine yield reached 97%. The catalyst showed excellent resistance to CO and sulfur poisoning. It also maintained structural stability after high-temperature reduction treatment at 600 °C, demonstrating the high robustness of the single-atom active sites. In addition to monometallic SACs, bimetallic SACs and single-atom alloy catalysts (SAACs) have also been developed to further enhance catalytic performance. Qi *et al.*[176] further designed a Ru–Co surface single-atom alloy (Ru_1CoNP/HAP) supported on hydroxyapatite (HAP). By atomically dispersing Ru onto the surface of Co nanoparticles, they achieved efficient cascade conversion of FF to piperidine. *In situ* characterization and theoretical calculations showed that the Ru_1CoNP structure promotes selective C–O bond cleavage of tetrahydrofurfurylamine (THFAM). This generates a 5-amino-1-pentanol intermediate, which then cyclizes and undergoes dehydration to form piperidine with a yield of 93%. The catalyst forms a stable single-atom alloy structure when the Co/Ru molar ratio is ≥10. This significantly inhibits side reaction pathways and demonstrates broad applicability for synthesiz-

Table 3 Other types of catalysts for selective production of NCCs

Type	Reactant	Catalyst	Nitrogen source and reductant	Temperature and time	Conversion	Ref.
Single-atom	HMF	Pd_1/BNC	NH_3 (0.2 MPa), isopropanol	80 °C, 6 h	100%	46
	HMF	Pd_1/BNC	NH_3 (0.2 MPa), methanol	80 °C, 6 h	100%	46
	HMF	Pd_1/BNC	NH_3 (0.2 MPa), ethanol	80 °C, 6 h	100%	46
	FF	Ru1/NC-900-800NH_3	NH_3 (0.5 MPa), H_2 (2 MPa)	100 °C, 10 h	>99%	148
	FF	Ru_1CoNP/HAP	NH_3 (0.5 MPa), H_2 (1 MPa)	100 °C, 6 h 180 °C, 14 h	>93%	176
Non-metallic	FF	HZSM-5 (Si/Al = 25)	75% NH_3–25% N_2	650 °C, 2.6 s	33.04% (yield)	21
	Cellulose	HZSM-5 (Si/Al = 83.3)	50% NH_3–50% N_2	500 °C, 5 min	40.64% (yield)	79
Hybrid	Benzaldehyde	Co_3ZnC–ZnO/NC-500 (MOF-derived)	Nitrobenzene, H_2 (1.8 MPa)	120 °C, 7 h	>99%	177
	Aryethylamines	Co-NPC/ZrO_2 (MOF-derived)	Aryethylamines	110 °C, 16 h	81% (yield)	178

ing pyridine and its derivatives. SACs, through the precise design of atomic-level active sites, have opened new pathways for the selective conversion of aldehydes and ketones into NCCs. Their core advantages lie in the optimization of reactant adsorption/desorption dynamics *via* coordination environment tuning, suppression of metal agglomeration and side reaction pathways, enhancement of selectivity and atom economy, as well as improved resistance to poisoning and cycling stability. Future research should focus on the scalable synthesis of SACs and the dynamic evolution mechanisms in complex reaction networks. Additionally, exploring collaborative integration strategies with other catalytic materials, such as zeolites and MOFs, will be crucial for promoting the industrial production of biomass-based NCCs.

5.2 Non-metallic and hybrid catalysts

In the research on the catalytic conversion of aldehyde and ketone carbonyl compounds to NCCs, non-metallic catalysts have demonstrated significant catalytic activity due to their unique acidity regulation ability and morphology selectivity. Zeolite catalysts, represented by HZSM-5, show high activity and selectivity in the ammoniation/amination reactions of biomass-derived aldehydes and ketones (such as FF, acetaldehyde, and acetone). This is due to their microporous structure and Brønsted acid centers. The Si/Al ratio of HZSM-5 directly affects its acid density and strength, which in turn regulates the reaction pathways. Yao *et al.*[21] found that a lower Si/Al ratio (such as 25) provides more strong acid sites, promoting the ammoniation of FF and other compounds with NH3 while suppressing coke formation. Under conditions of 650 °C and 75% NH_3–25% N_2, HZSM-5 (Si/Al = 25) increased the indole carbon yield to 33.04%. In addition, the microporous structure of HZSM-5 (~0.55 nm) restricts the diffusion of large molecular intermediates. This promotes the formation of small NCCs, such as pyrrole and pyridine. These compounds then undergo Diels–Alder cycloaddition or ring-opening reactions to form indole.[20]

In co-catalytic pyrolysis systems, HZSM-5 demonstrates a significant synergistic catalytic effect. When cellulose is co-pyrolyzed with polyoxymethylene, the formaldehyde produced from the pyrolysis of polyoxymethylene acts as an alkylation reagent. It reacts with cellulose-derived products (such as light oxygenated compounds) to form methyl-substituted pyridine, increasing the total yield of pyridine by 40.64%.[79] This synergistic effect not only enhances the diversity of NCCs but also reduces the formation of by-products by *in situ* utilization of intermediates. It is worth noting that HZSM-5 exhibited good stability in these studies, showing only a 5.5% loss in indole yield after 5 reaction-regeneration cycles in a diluted NH_3 environment. However, in a pure NH_3 environment, the loss was as high as 25.5%.[21] Characterization analysis shows that diluted NH_3 can slow down alumina loss and the depletion of acidic sites, maintaining the catalyst's microporous structure and acid density.[20] It is clear that non-metallic catalysts like HZSM-5, through the synergistic action of acidic sites and pore structure, can efficiently catalyze the conversion of aldehyde and ketone compounds into high-value NCCs. They also show great potential for application in complex feedstock systems and industrial scale-up.

As a representative of composite catalysts, the intrinsic properties of MOF materials make their application in catalysis cross-category. In the "Metal catalysts" section, MOFs are primarily mentioned for their catalytic behavior driven by metal active sites, such as metal nodes or single-atom metals. She *et al.*[177] developed a Co/Zn bimetallic MOF-derived Co_3ZnC–ZnO/NC-500 catalyst for the one-pot conversion of nitroaromatic compounds and aromatic aldehydes (Fig. 14). Through a pyrolysis strategy, the MOF precursor is converted into a nitrogen-doped carbon nanosheet-supported Co_3ZnC alloy and ZnO composite structure. Its high specific surface area (105.5 $m^2 g^{-1}$) and abundant defect sites significantly enhance the conversion rate of nitrobenzene (99.9%) and imine selectivity (98.5%). Additionally, the presence of ZnO effectively suppresses the over-hydrogenation of imines by regulating the adsorption of active hydrogen species. The synergistic effect between Co_3ZnC alloy and nitrogen-doped carbon accelerates the tandem process of nitro reduction and imine-aldehyde condensation. This demonstrates the precise control capability of MOF-derived composite catalysts in tandem reactions. When mentioning non-metallic catalysts, the composite nature of MOF is reflected in its deep integration with non-metallic components. Xian *et al.*[178] developed a MOF-derived N, P co-doped carbon-supported single-atom cobalt catalyst. Through a surface functionalization strategy, they combined the atomically dispersed CoN_3P_1 active sites with the carbon-based support, forming a composite system with a hierarchical pore structure and high surface area. The catalyst activates oxygen through the atomically dispersed CoN_3P_1 sites, facilitating the deamination oxidation of phenyl ethylamine to form a 1,2-diketone intermediate. This intermediate then undergoes condensation and cyclization with free amines, efficiently synthesizing polysubstituted imidazole compounds with a maximum yield of 81%. Non-metallic and composite catalysts exhibit unique advantages and application potential in the catalytic conversion of aldehyde and ketone compounds. Exploring the structure–activity relationship optimization of non-metallic and composite catalysts, along with in-depth analysis of reaction mechanisms, can further enhance catalytic efficiency and selectivity for target products, offering new strategies for the efficient conversion of biomass-derived carbonyl compounds.

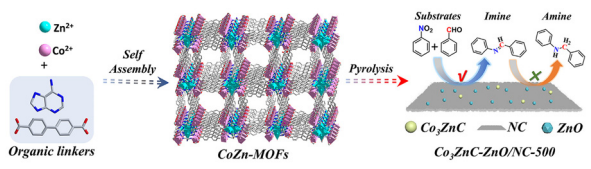

Fig. 14 Schematic of the synthesis strategy for Co3ZnC–ZnO/NC-500 catalyst derived from Co/Zn bimetallic MOF.[177]

6. Conclusions and outlook

Biomass, with its dual carbon and nitrogen potential, offers unique advantages over fossil resources for producing NHCs. This review systematically summarizes the research progress on the conversion of biomass-derived aldehyde and ketone platform compounds into NHCs, with a focus on the key role of catalysts in pathway regulation and selectivity optimization. Compared with prior reviews focusing on individual catalytic systems or simplified model reactions, this work uniquely emphasizes the reaction pathway competition in multicomponent biomass systems and integrates mechanistic analysis, thermodynamic evaluation, and catalyst design perspectives to construct a systematic understanding. This review first categorizes the catalytic transformation of aldehyde and ketone platform compounds (*e.g.*, FF, HMF, acetone) into NHCs such as pyridine and pyrrole *via* ammonia addition, reductive amination, and cyclization. Due to the complexity of biomass-derived functionalities, pathway competition and side reactions significantly affect selectivity and yield. Catalytic strategies based on acidic zeolites, transition metals, and multifunctional systems have shown promise in enhancing pathway control. The integration of catalyst design with kinetic modeling provides a basis for steering nitrogen incorporation pathways, and offers synergy with studies on MOF- or transition metal-based systems. However, current technologies still face challenges such as low selectivity (<50%), complex product mixtures, and excessive hydrogenation side reactions induced by noble metals like Pt and Pd. Additionally, competing reaction mechanisms in the system (such as condensation, deoxygenation, and nitration pathways running in parallel) reduce the yield of target products. Future progress should leverage complementary advances in data-driven catalyst screening and *in situ* characterization, while fostering collaboration between mechanistic and process-oriented studies. To address these issues, future research should focus on the following directions:

Catalyst design precision: develop non-noble metal catalysts with "confinement effects" or dual active sites (such as transition metal sulfides or nitrogen-doped carbon-based materials) to differentially regulate the hydrogenation and condensation pathways of aldehyde and ketone functional groups. This will help suppress side reactions like furan ring opening and promote the efficient formation of C–N and C=N bonds.

Dynamic reaction mechanism analysis: combine various *in situ* characterization techniques with mass spectrometry, along with DFT computational chemistry simulations. This approach aims to reveal the dynamic evolution paths of aldehyde and ketone intermediates in the pyrolysis-nitration coupling process. It will clarify the kinetic differences in the formation of products like pyridine and pyrrole, providing data support for pathway optimization.

Process optimization and integration: develop a "hierarchical pyrolysis-catalytic nitration" coupling system. This system uses temperature gradients to achieve *in situ* enrichment and directional conversion of aldehyde and ketone intermediates, simplifying product distribution and improving yield.

High-value application expansion: for specific high-value products like pyridine-based pesticides and fluorescent pyrrole derivatives, establish a "feedstock-process-performance" correlation model to promote the practical application of biomass-derived chemicals in pharmaceuticals and functional materials.

Unlike previous reviews that focus on single catalyst systems or isolated reaction routes, this study provides an integrated perspective on multicomponent reaction networks, catalyst–substrate interactions, and kinetic and thermodynamic control. By connecting mechanistic understanding with catalytic optimization, it identifies key challenges that require coordinated efforts. While recent studies have advanced NHC synthesis from biomass-derived intermediates, they largely focus on pure substrates under idealized conditions. In contrast, this review emphasizes complex feedstocks and pathway competition, offering insights more applicable to real-world catalytic design. Future progress will benefit from data-driven approaches—such as kinetic modeling and AI-guided screening—as well as collaborative benchmarking to unify performance standards and accelerate technological advancement. In summary, the synthesis of biomass-derived NHCs supports carbon neutrality goals and the full valorization of biomass. This review provides insights to guide future catalyst exploration and promotes efficient, sustainable chemical production from renewable resources.

Author contributions

Zhisen He: writing – original draft, conceptualization, methodology. Shanjian Liu: writing – review & editing, funding acquisition, resources. Fernando Cardenas-Lizana: investigation, methodology. Dongmei Bi: writing – review & editing, funding acquisition, project administration. Aimaro Sanna: writing – review & editing, funding acquisition, supervision.

Conflicts of interest

There are no conflicts to declare.

Data availability

No primary research results, software or code have been included and no new data were generated or analysed as part of this review.

Acknowledgements

This work was supported by the National Natural Science Foundation of China (no. 52176193), the China Scholarship Council (202401040004), Shandong Innovation Fund for Small and Medium-sized Technology-based Firms (no. 2023TSGC0983) and Innovate UK (KTP 10129935).

References

1 P. Yogheshwari, P. Karuppasamy, M. S. Pandian, P. Ramasamy and K. Anitha, *J. Mol. Struct.*, 2022, **1270**, 133884.
2 Y. Zhu, K. Liao, Y. Li, W. Zhang, B. Song, X.-Q. Hao and X. Zhu, *Dyes Pigm.*, 2024, **224**, 112004.
3 X. Zhang, Y. Li, Y. Huo, L. Guo, C. Wu and Z. Wu, *Microporous Mesoporous Mater.*, 2020, **306**, 110442.
4 Z. Chen, L. Chen, K. S. Khoo, V. K. Gupta, M. Sharma, P. L. Show and P.-S. Yap, *Biotechnol. Adv.*, 2023, **69**, 108265.
5 D. Bi, Z. He, F. Huang, G. Zhang, H. Wang and S. Liu, *Chem. Eng. J.*, 2024, **496**, 153798.
6 Z. He, S. Liu, W. Zhao, J. Liu and D. Bi, *J. Anal. Appl. Pyrolysis*, 2023, **175**, 106219.
7 H. Zou and J. Chen, *Appl. Catal., B*, 2022, **309**, 121262.
8 X. Luo, Y. Li, N. K. Gupta, B. Sels, J. Ralph and L. Shuai, *Angew. Chem., Int. Ed.*, 2020, **59**, 11704–11716.
9 Y. Meng, J. S. Huang, J. Li, Y. M. Jian, S. Yang and H. Li, *Green Chem.*, 2023, **25**, 4453–4462.
10 F. Xu, Z. Li, L. L. Zhang, S. Q. Liu, H. Li, Y. H. Liao and S. Yang, *Green Chem.*, 2023, **25**, 3297–3305.
11 Q. Yan, X. Wu, H. Jiang, H. Wang, F. Xu, H. Li, H. Zhang and S. Yang, *Coord. Chem. Rev.*, 2024, **502**, 215622.
12 Y. Zhong, F. Liu, J. Li and C. Guo, *Green Chem.*, 2024, **26**, 11019–11060.
13 K. Zhao, B. Wen, Q. Tang, F. Wang, X. Liu, Q. Xu and D. Yin, *Green Chem.*, 2024, **26**, 9957–9992.
14 C. Dong, H. Wang, H. Du, J. Peng, Y. Cai, S. Guo, J. Zhang, C. Samart and M. Ding, *Mol. Catal.*, 2020, **482**, 110755.
15 D. Luo, Y. He, X. Yu, F. Wang, J. Zhao, W. Zheng, H. Jiao, Y. Yang, Y. Li and X. Wen, *J. Catal.*, 2021, **395**, 293–301.
16 Z. He, A. Zhao, S. Liu, Y. Chen, J. Liu, W. Zhao, M. Yin, Q. Dong, J. Zhang, G. Zhang and D. Bi, *Chem. Eng. J.*, 2024, **496**, 153793.
17 S. Liu, W. Zhao, Z. He, M. Yin, J. Yao and W. Yi, *J. Energy Inst.*, 2024, **113**, 101501.
18 L. Xu, Q. Yao, Z. Han, Y. Zhang and Y. Fu, *ACS Sustainable Chem. Eng.*, 2016, **4**, 1115–1122.
19 S. Song, V. F. K. Yuen, L. Di, Q. Sun, K. Zhou and N. Yan, *Angew. Chem., Int. Ed.*, 2020, **59**, 19846–19850.
20 Q. Yao, L. Xu, Z. Han and Y. Zhang, *Chem. Eng. J.*, 2015, **280**, 74–81.
21 Q. Yao, L. Xu, Y. Zhang and Y. Fu, *J. Anal. Appl. Pyrolysis*, 2016, **121**, 258–266.
22 B. L. Yin, X. Y. Zhang, X. T. Zhang, H. Peng, W. Zhou, B. Liu and H. F. Jiang, *Chem. Commun.*, 2015, **51**, 6126–6129.
23 L. J. Xu, Q. Yao, Y. Zhang and Y. Fu, *RSC Adv.*, 2016, **6**, 86034–86042.
24 L. J. Xu, Z. Han, Q. Yao, J. Deng, Y. Zhang, Y. Fu and Q. X. Guo, *Green Chem.*, 2015, **17**, 2426–2435.
25 B. Wozniak, Y. Li, S. Hinze, S. Tin and J. G. de Vries, *Eur. J. Org. Chem.*, 2018, 2009–2012.
26 W. Jia, H. Liu, Y. Feng, J. Zhang, X. Zhao, Y. Sun, Z. Wei, S. Yang, X. Tang, X. Zeng and L. Lin, *J. Cleaner Prod.*, 2022, **345**, 131029.
27 Z. W. Jiang, Y. J. Zeng, D. Hu, R. C. Guo, K. Yan and R. Luque, *Green Chem.*, 2023, **25**, 871–892.
28 J. Zhang, J. Yin, X. Duan, C. Zhang and J. Zhang, *J. Catal.*, 2023, **420**, 89–98.
29 P. Mäki-Arvela, I. L. Simakova and D. Y. Murzin, *Catal. Rev. Sci. Eng.*, 2023, **65**, 501–568.
30 K. Murugesan, T. Senthamarai, V. G. Chandrashekhar, K. Natte, P. C. J. Kamer, M. Beller and R. V. Jagadeesh, *Chem. Soc. Rev.*, 2020, **49**, 6273–6328.
31 J. Yang, C. Yao, J. Luo, J. Shan, J. Liu, C. Lu, F. Feng, Q. Zhang, Q. Wang and X. Li, *Mol. Catal.*, 2024, **563**, 114254.
32 L. Leng, L. Yang, J. Chen, S. Leng, H. Li, H. Li, X. Yuan, W. Zhou and H. Huang, *Bioresour. Technol.*, 2020, **315**, 123801.
33 Z. Du, B. Hu, X. Ma, Y. Cheng, Y. Liu, X. Lin, Y. Wan, H. Lei, P. Chen and R. Ruan, *Bioresour. Technol.*, 2013, **130**, 777–782.
34 X. Wang, X. Tang and X. Yang, *Energy Convers. Manage.*, 2017, **140**, 203–210.
35 X. Y. Zhao, W. Jiang, Y. F. Shan and J. P. Cao, *Energy Fuels*, 2022, **36**, 502–513.
36 Z. Ma, Y. Zhang, C. Li, Y. Yang, W. Zhang, C. Zhao and S. Wang, *Bioresour. Technol.*, 2019, **292**, 122034.
37 D. Li, M. Fu, T. Pei, Y. Lu, C. Liu, X. Lin, D. Hou, H. Sun, C. Luo, Z. Zheng and Y. Zheng, *J. Environ. Chem. Eng.*, 2023, **11**, 110093.
38 X. Zhang, Z. Yuan, Q. Yao, Y. Zhang and Y. Fu, *Bioresour. Technol.*, 2019, **290**, 121800.
39 B. Qiu, X. Tao, Y. Wang, D. Zhang and H. Chu, *Green Energy Environ.*, 2024, DOI: **10.1016/j.gee.2024.11.009**.
40 G. Dai, X. Li, H. Lin, Y. Zhang, Z. Hu, J. Zhang, H. Tan and X. Wang, *Fuel*, 2024, **376**, 132689.
41 P. Wang, C. Shen, B. Wang, P. Xu and L. Shen, *Fuel*, 2022, **326**, 125071.
42 N. S. Gould, H. Landfield, B. Dinkelacker, C. Brady, X. Yang and B. Xu, *ChemCatChem*, 2020, **12**, 2106–2115.
43 K. Murugesan, M. Beller and R. V. Jagadeesh, *Angew. Chem., Int. Ed.*, 2019, **58**, 5064–5068.
44 Y. Xu, J. Zhang, P. Wang, Y. Fan, Y. Jiang, X. Duan, Y. Li and J. Zhang, *Chem. Eng. J.*, 2024, **480**, 148175.
45 J. F. Chen, X. Gong, J. Y. Li, Y. K. Li, J. G. Ma, C. K. Hou, G. Q. Zhao, W. C. Yuan and B. G. Zhao, *Science*, 2018, **360**, 1438.
46 W. J. Liu, X. Zhou, Y. Min, J. W. Huang, J. J. Chen, Y. Wu and H. Q. Yu, *Adv. Mater.*, 2024, **36**, 2305924.
47 K. Wang, Z. H. Deng, S. J. Xie, D. D. Zhai, H. Y. Fang and Z. J. Shi, *Nat. Commun.*, 2021, **12**, 248.
48 J. Zhang, X. Yang, Z. Jia, Q. Han, S. Yu, S. Liu, L. Li, Q. Wu, H. Yu, Y. Liu and Y. Liu, *Chem. Eng. J.*, 2024, **500**, 157400.
49 Y. Gao, H. Zhao, J. Liang, C. Liu, H. Yuan, Y. Zheng, H. Li, F. Wang and Z. Dong, *Chem. Eng. J.*, 2025, **503**, 158045.

50 G. D. Yadav and R. K. Mewada, *Catal. Today*, 2012, **198**, 330–337.
51 Z. Zhang, R. Liu, L. Huang and P. Liu, *J. Catal.*, 2024, **440**, 115824.
52 L. Hu, A. Y. He, X. Y. Liu, J. Xia, J. X. Xu, S. Y. Zhou and J. M. Xu, *ACS Sustainable Chem. Eng.*, 2018, **6**, 15915–15935.
53 X. F. Wang, X. H. Liang, J. M. Li and Q. B. Li, *Appl. Catal., A*, 2019, **576**, 85–95.
54 A. Messori, A. Fasolini and R. Mazzoni, *ChemSusChem*, 2022, **15**, e202200228.
55 L. Hu, L. Lin, Z. Wu, S. Y. Zhou and S. J. Liu, *Renewable Sustainable Energy Rev.*, 2017, **74**, 230–257.
56 J. Zhang, D.-n. Li, H.-r. Yuan, S.-r. Wang and Y. Chen, *J. Fuel Chem. Technol.*, 2021, **49**, 1752–1766.
57 J. Su, X. Yang, H. Shi, S. Yao and M. Zhou, *J. Colloid Interface Sci.*, 2024, **669**, 336–348.
58 T. Cai, L. Yao, J. Fan and H. Peng, *J. Taiwan Inst. Chem. Eng.*, 2023, **146**, 104870.
59 A. Tampieri, K. Föttinger, N. Barrabés and F. Medina, *Appl. Catal., B*, 2022, **319**, 121889.
60 R. Balaga, P. Yan, K. Ramineni, H. Du, Z. Xia, M. R. Marri and Z. C. Zhang, *Appl. Catal., A*, 2022, **648**, 118901.
61 R. Mariscal, P. Maireles-Torres, M. Ojeda, I. Sádaba and M. L. Granados, *Energy Environ. Sci.*, 2016, **9**, 1144–1189.
62 J. He, Q. Qiang, S. Liu, K. Song, X. Zhou, J. Guo, B. Zhang and C. Li, *Fuel*, 2021, **306**, 121765.
63 T. Y. Deng and B. H. Yan, *Green Chem.*, 2022, **24**, 6860–6866.
64 R. Q. Raguindin, M. N. Gebresillase, J. Kang, Y.-W. Suh and J. G. Seo, *Bioresour. Technol.*, 2025, **416**, 131764.
65 S. Shao, X. Xia, X. Li, H. Zhang and R. Xiao, *Fuel Process. Technol.*, 2023, **250**, 107904.
66 X. Li, B. Feng, H. Zhang, Y. Liu, M. Xiao, T. Huang, Q. Zhu and H. Song, *Fuel*, 2025, **380**, 133140.
67 H. Wang, L. Liu, J. Bian and C. Li, *J. Fuel Chem. Technol.*, 2024, **52**, 1617–1628.
68 D. Ouyang, D. Gao, J. Hong, Z. Jiang and X. Zhao, *J. Energy Chem.*, 2023, **79**, 135–147.
69 L. J. Xu, Y. Y. Jiang, Q. Yao, Z. Han, Y. Zhang, Y. Fu, Q. X. Guo and G. W. Huber, *Green Chem.*, 2015, **17**, 1281–1290.
70 P. Gallezot, *Chem. Soc. Rev.*, 2012, **41**, 1538–1558.
71 Q. A. Lu, Z. F. Zhang, C. Q. Dong and X. F. Zhu, *Energies*, 2010, **3**, 1805–1820.
72 C. Moreau, M. N. Belgacem and A. Gandini, *Top. Catal.*, 2004, **27**, 11–30.
73 P. Lejemble, A. Gaset and P. Kalck, *Biomass*, 1984, **4**, 263–274.
74 D. Z. Ren, X. L. Jiang, N. H. Zhang, J. Duo, K. Norinaga and Z. B. Huo, *Biomass Convers. Biorefin.*, 2023, **13**, 8115–8121.
75 R. J. van Putten, J. C. van der Waal, E. de Jong, C. B. Rasrendra, H. J. Heeres and J. G. de Vries, *Chem. Rev.*, 2013, **113**, 1499–1597.
76 C. C. Truong, D. K. Mishra and Y. W. Suh, *ChemSusChem*, 2023, **16**, e202201846.
77 J. He, L. L. Chen, S. M. Liu, K. Song, S. Yang and A. Riisager, *Green Chem.*, 2020, **22**, 6714–6747.
78 L. J. Xu, Q. Yao, J. Deng, Z. Han, Y. Zhang, Y. Fu, G. W. Huber and Q. X. Guo, *ACS Sustainable Chem. Eng.*, 2015, **3**, 2890–2899.
79 X. Zhou, L. Jiang, H. Zhang, C. Dong and L. Xu, *J. Anal. Appl. Pyrolysis*, 2021, **158**, 105275.
80 C.-W. Luo, X.-Y. Feng, W. Liu, X.-Y. Lia and Z.-S. Chao, *Microporous Mesoporous Mater.*, 2016, **235**, 261–269.
81 N. G. Grigorieva, S. A. Kostyleva, S. V. Bubennov, V. R. Bikbaeva, A. R. Gataulin, N. A. Filippova, A. N. Khazipova, T. R. Prosochkina, B. I. Kutepov and N. Nama, *J. Saudi Chem. Soc.*, 2019, **23**, 452–460.
82 N. G. Grigor'eva, M. R. Agliullin, S. A. Kostyleva, S. V. Bubennov, V. R. Bikbaeva, A. R. Gataulin, N. A. Filippova, B. I. Kutepov and N. Narender, *Kinet. Catal.*, 2019, **60**, 733–743.
83 Y. S. Higasio and T. Shoji, *Appl. Catal., A*, 2001, **221**, 197–207.
84 P. Kalck and M. Urrutigöity, *Chem. Rev.*, 2018, **118**, 3833–3861.
85 J. S. Barber, M. M. Yamano, M. Ramirez, E. R. Darzi, R. R. Knapp, F. Liu, K. N. Houk and N. K. Garg, *Nat. Chem.*, 2018, **10**, 953–960.
86 Y. M. Questell-Santiago, M. V. Galkin, K. Barta and J. S. Luterbacher, *Nat. Rev. Chem.*, 2020, **4**, 311–330.
87 L. Ke, Q. Wu, N. Zhou, J. Xiong, Q. Yang, L. Zhang, Y. Wang, L. Dai, R. Zou, Y. Liu, R. Ruan and Y. Wang, *Renewable Sustainable Energy Rev.*, 2022, **165**, 112607.
88 B. Bissaro, E. Kommedal, Å. Rohr and V. G. H. Eijsink, *Nat. Commun.*, 2020, **11**, 890.
89 G. Zhu, X. Qiu, Y. Zhao, Y. Qian, Y. Pang and X. Ouyang, *Bioresour. Technol.*, 2016, **218**, 718–722.
90 X. C. Dai, X. Z. Wang, J. Rabeah, C. Kreyenschulte, A. Brückner and F. Shi, *Chem. – Eur. J.*, 2021, **27**, 16889–16895.
91 G. F. Liang, A. Q. Wang, L. Li, G. Xu, N. Yan and T. Zhang, *Angew. Chem., Int. Ed.*, 2017, **56**, 3050–3054.
92 V. Froidevaux, C. Negrell, S. Caillol, J. P. Pascault and B. Boutevin, *Chem. Rev.*, 2016, **116**, 14181–14224.
93 T. Irrgang and R. Kempe, *Chem. Rev.*, 2020, **120**, 9583–9674.
94 S. J. Kulkarni, R. R. Rao, M. Subrahmanyam and A. V. R. Rao, *Appl. Catal., A*, 1994, **113**, 1–7.
95 H. D. Chu, X. Q. Feng, X. Wu, J. T. Song, C. Shen and T. W. Tan, *ACS Sustainable Chem. Eng.*, 2023, **11**, 177–186.
96 M. Wang, M. A. Khan, I. Mohsin, J. Wicks, A. H. Ip, K. Z. Sumon, C. T. Dinh, E. H. Sargent, I. D. Gates and M. G. Kibria, *Energy Environ. Sci.*, 2021, **14**, 2535–2548.
97 R. Wang, Y. T. Liu, G. Y. Li, A. Q. Wang, X. D. Wang, Y. Cong, T. Zhang and N. Li, *ACS Catal.*, 2021, **11**, 4810–4820.
98 T. J. Peglow, G. P. d. Costa, L. F. B. Duarte, M. S. Silva, T. Barcellos, G. Perin and D. Alves, *J. Org. Chem.*, 2019, **84**, 5471–5482.
99 M. L. Hua, J. L. Song, X. Huang, M. Q. Hou, H. L. Fan, Z. F. Zhang, T. B. Wu and B. X. Han, *ACS Catal.*, 2021, **11**, 7685–7693.

100 Q. A. Wang, C. F. Wan, Y. Gu, J. T. Zhang, L. F. Gao and Z. Y. Wang, *Green Chem.*, 2011, **13**, 578–581.
101 H. Sharma, N. Singh and D. O. Jang, *Green Chem.*, 2014, **16**, 4922–4930.
102 A. S. Makarov, A. A. Merkushev, M. G. Uchuskin and I. V. Trushkov, *Org. Lett.*, 2016, **18**, 2192–2195.
103 X. Chen, S. Song, H. Y. Li, G. Gözaydin and N. Yan, *Acc. Chem. Res.*, 2021, **54**, 1711–1722.
104 M. Chatterjee, T. Ishizaka and H. Kawanami, *Green Chem.*, 2016, **18**, 487–496.
105 S. Nishimura, K. Mizuhori and K. Ebitani, *Res. Chem. Intermed.*, 2016, **42**, 19–30.
106 C. Lin, L. Xu, Y. Zhuang, P. Ma, H. Wu, H. Gan, F. Cao and P. Wei, *Chem. Eng. Sci.*, 2025, **305**, 121099.
107 Y. Wang, M. T. Chen, K. Y. Zhang, H. M. Wu, J. L. Wang, Y. R. Cheng, Y. X. Liu and Z. J. Wei, *ACS Catal.*, 2023, **13**, 12601–12616.
108 A. Bellè, T. Tabanelli, G. Fiorani, A. Perosa, F. Cavani and M. Selva, *ChemSusChem*, 2019, **12**, 3343–3354.
109 P. Barbaro, F. Liguori, C. Oldani and C. Moreno-Marrodán, *Adv. Sustainable Syst.*, 2020, **4**, 1900117.
110 Y. Wei, Z. Sun, Q. Li, D. Wu, J. Wang, Y. Zhang, C. C. Xu and R. Nie, *Fuel*, 2024, **369**, 131703.
111 Y. Wei, K. You, W. Xu, F. Zhao, D. Yan, X. Zhang, Z. Chen and H. a. Luo, *Appl. Catal., A*, 2024, **685**, 119885.
112 M. Zhang, Z. Liu, Y. Yan, D. Liu, G. Xu, Y. An, Y. Zou, Y. Yu, J. S. Francisco and H. He, *Nat. Commun.*, 2025, **16**, 1943.
113 Y. Ni, R. Zhao, M. Jiang, D. Bi, J. Ma and Y. Li, *Sep. Purif. Technol.*, 2025, **359**, 130604.
114 G. Zhang, S. Liu, D. Yao, Z. Qin, Z. He and D. Bi, *Ind. Crops Prod.*, 2024, **219**, 119091.
115 S. Özkınalı, M. S. Çavuş, T. Tosun, N. Şener, M. Gür and İ. Şener, *J. Mol. Struct.*, 2025, **1325**, 140901.
116 R. Pogorevc, B. Hočevar, M. Grilc and B. Likozar, *Chem. Eng. J.*, 2025, **505**, 159527.
117 X. Z. Zhuang, J. G. Liu, S. R. Zhong and L. L. Ma, *Green Chem.*, 2022, **24**, 271–284.
118 L. Gou, L. F. Xie, Y. Y. Wang and L. Y. Dai, *Appl. Catal., A*, 2022, **647**, 118902.
119 J. J. Wang, G. N. Li, Z. L. Li, C. Z. Tang, Z. C. Feng, H. Y. An, H. L. Liu, T. F. Liu and C. Li, *Sci. Adv.*, 2017, **3**, 1701290.
120 Y. F. Feng, Y. Men, W. Liu, Y. J. Hu and J. G. Wang, *Colloids Surf., A*, 2024, **701**, 134977.
121 R. P. Ye, J. Ding, T. R. Reina, M. S. Duyar, H. T. Li, W. H. Luo, R. B. Zhang, M. H. Fan, G. Feng, J. Sun and J. Liu, *Nat. Synth.*, 2025, **4**, 288–302.
122 J. H. Hu, W. J. Deng, J. F. Zhou and Y. B. Huang, *Nat. Commun.*, 2025, **16**, 1029.
123 N. Guo, S. Caratzoulas, D. J. Doren, S. I. Sandler and D. G. Vlachos, *Energy Environ. Sci.*, 2012, **5**, 6703–6716.
124 A. H. Motagamwala and J. A. Dumesic, *Chem. Rev.*, 2021, **121**, 1049–1076.
125 G. R. Wittreich, K. Alexopoulos and D. G. Vlachos, in *Handbook of Materials Modeling: Applications: Current and Emerging Materials*, Springer, 2020, pp. 1377–1404.
126 M. Usman, D. Cresswell and A. Garforth, *Ind. Eng. Chem. Res.*, 2012, **51**, 158–170.
127 Z. Rao, G. Shi, Z. Wang, A. Mahmood, X. Xie and J. Sun, *Chem. Eng. J.*, 2020, **395**, 125078.
128 P. Xu, C. Ding, Z. Li, R. Yu, H. Cui and S. Gao, *Chemosphere*, 2023, **319**, 137995.
129 S. L. Jiao, X. W. Fu and H. W. Huang, *Adv. Funct. Mater.*, 2022, **32**, 2107651.
130 N. G. Asenjo, R. Santamaría, C. Blanco, M. Granda, P. Álvarez and R. Menéndez, *Carbon*, 2013, **55**, 62–69.
131 T. Wang, J. Li, L. Shi and X. Dai, *J. Environ. Chem. Eng.*, 2025, **13**, 115393.
132 D. Y. Murzin, *Chem. Eng. Sci.*, 2022, **256**, 117684.
133 G. L. Xu, R. Wang, F. Yang, D. W. Ma, Z. X. Yang and Z. S. Lu, *Carbon*, 2017, **118**, 35–42.
134 X. Yan, C. Duan, R. Sun, X. Ji, Y. Zhang and H. Chu, *Fuel*, 2024, **369**, 131739.
135 W. Chen, X. Shi, X. Tao, W. Guo, Y. Wang, S. Deng, M. Gong, Y. Chen and H. Yang, *Fuel*, 2024, **361**, 130686.
136 D. Xu, J. Lin, R. Ma and S. Sun, *Fuel*, 2025, **384**, 133954.
137 L. Jiao, D. F. Zhang, Z. J. Hao, F. H. Yu and X. J. Lv, *ACS Catal.*, 2021, **11**, 8727–8735.
138 M. Xu, X. T. Qin, Y. Xu, X. C. Zhang, L. R. Zheng, J. X. Liu, M. Wang, X. Liu and D. Ma, *Nat. Commun.*, 2022, **13**, 6720.
139 J. Cueto, L. Faba, E. Díaz and S. Ordóñez, *Ind. Crops Prod.*, 2022, **188**, 115692.
140 M. H. Zhang, R. S. Li, Y. F. Wu and Y. Z. Yu, *Ind. Eng. Chem. Res.*, 2021, **60**, 2871–2880.
141 N. Gaggero and S. Pandini, *Org. Biomol. Chem.*, 2017, **15**, 6867–6887.
142 J. Cueto, D. de la Calle, M. d. Mar Alonso-Doncel, E. A. Giner, R. A. García-Muñoz and D. P. Serrano, *Bioresour. Technol.*, 2025, **418**, 131877.
143 M. A. Ashley and T. Rovis, *J. Am. Chem. Soc.*, 2020, **142**, 18310–18316.
144 B. D. Dherange, M. B. Yuan, C. B. Kelly, C. A. Reiher, C. Grosanu, K. J. Berger, O. Gutierrez and M. D. Levin, *J. Am. Chem. Soc.*, 2023, **145**, 17–24.
145 W. H. Li, W. X. Duan, Q. X. Tang, Z. T. Li and G. Y. Yang, *Green Chem.*, 2021, **23**, 1136–1139.
146 M. Shang, M. Cao, Q. F. Wang and M. Wasa, *Angew. Chem., Int. Ed.*, 2017, **56**, 13338–13341.
147 S. Zhang, Z. M. Xia, Y. Zou, M. K. Zhang and Y. Q. Qu, *Nat. Commun.*, 2021, **12**, 3382.
148 H. F. Qi, J. Yang, F. Liu, L. L. Zhang, J. Y. Yang, X. Y. Liu, L. Li, Y. Su, Y. F. Liu, R. Hao, A. Q. Wang and T. Zhang, *Nat. Commun.*, 2021, **12**, 3295.
149 Z. W. Xu, P. F. Yan, W. J. Xu, S. Y. Jia, Z. Xia, B. Chung and Z. C. Zhang, *RSC Adv.*, 2014, **4**, 59083–59087.
150 Z. W. Xu, P. F. Yan, K. R. Liu, L. Wan, W. J. Xu, H. X. Li, X. M. Liu and Z. C. Zhang, *ChemSusChem*, 2016, **9**, 1255–1258.
151 X. Y. Li, S. D. Le and S. Nishimura, *Catal. Lett.*, 2022, **152**, 2860–2868.

152 D. Chandra, Y. Inoue, M. Sasase, M. Kitano, A. Bhaumik, K. Kamata, H. Hosono and M. Hara, *Chem. Sci.*, 2018, **9**, 5949–5956.
153 H. Wang, Y. Zhang, D. Luo, H. Wang, Y. He, F. Wang and X. Wen, *Mol. Catal.*, 2023, **536**, 112914.
154 M. Ronda-Leal, C. Espro, N. Lazaro, M. Selva, A. Perosa, S. M. Osman, A. Pineda, R. Luque and D. Rodríguez-Padrón, *Mater. Today Chem.*, 2022, **24**, 100873.
155 Z. Y. Wang, Y. J. Zheng, J. Y. Feng, W. B. Zhang and Q. S. Gao, *Chem. – Eur. J.*, 2023, **29**, e202300947.
156 M. K. Zhang, Y. Zou, S. Zhang and Y. Q. Qu, *ChemCatChem*, 2022, **14**, e202200176.
157 A. García-Ortiz, J. D. Vidal, M. J. Climent, P. Concepción, A. Corma and S. Iborra, *ACS Sustainable Chem. Eng.*, 2019, **7**, 6243–6250.
158 K. Zhou, H. Y. Liu, H. M. Shu, S. W. Xiao, D. C. Guo, Y. X. Liu, Z. J. Wei and X. N. Li, *ChemCatChem*, 2019, **11**, 2649–2656.
159 W. Song, Y. Wan, Y. Li, X. Luo, W. Fang, Q. Zheng, P. Ma, J. Zhang and W. Lai, *Catal. Sci. Technol.*, 2022, **12**, 7208–7218.
160 Q. Z. Hu, S. Jiang, Y. Wu, H. Z. Xu, G. Q. Li, Y. Zhou and J. Wang, *ChemSusChem*, 2022, **15**, e202200192.
161 P. Liu, X. L. Li, H. Y. Zhang, Y. C. Zhang and J. Q. Zhao, *J. Catal.*, 2024, **429**, 115291.
162 Y. Yang, L. Zhou, X. Wang, L. Zhang, H. Cheng and F. Zhao, *Nano Res.*, 2023, **16**, 3719–3729.
163 Y. Yang, L. Zhang, L. Zhou, H. Cheng and F. Zhao, *Chem. Res. Chin. Univ.*, 2024, **40**, 36–46.
164 R. Sun, L. Xiao and W. Wu, *Mol. Catal.*, 2024, **553**, 113710.
165 Y. Wan, P. Ma, H. Lu, J. Zhang, J. Wang, W. Fang, W. Song, Q. Zheng and W. Lai, *J. Catal.*, 2024, **429**, 115285.
166 V. G. Chandrashekhar, K. Natte, A. M. Alenad, A. S. Alshammari, C. Kreyenschulte and R. V. Jagadeesh, *ChemCatChem*, 2022, **14**, e202101234.
167 M. Sheng, S. Fujita, S. Yamaguchi, J. Yamasaki, K. Nakajima, S. Yamazoe, T. Mizugaki and T. Mitsudome, *JACS Au*, 2021, **1**, 501–507.
168 K. Zhou, B. Chen, X. Zhou, S. Kang, Y. Xu and J. Wei, *ChemCatChem*, 2019, **11**, 5562–5569.
169 Yogita, K. T. V. Rao, P. M. Kumar and N. Lingaiah, *Sustainable Energy Fuels*, 2022, **6**, 4692–4705.
170 Z. J. Wei, Y. R. Cheng, K. Zhou, Y. Zeng, E. Yao, Q. Li, Y. X. Liu and Y. Sun, *ChemSusChem*, 2021, **14**, 2308–2312.
171 X. Wang, W. Chen, Z. Li, X. Zeng, X. Tang, Y. Sun, T. Lei and L. Lin, *J. Energy Chem.*, 2018, **27**, 209–214.
172 T. Senthamarai, V. G. Chandrashekhar, M. B. Gawande, N. V. Kalevaru, R. Zbořil, P. C. J. Kamer, R. V. Jagadeesh and M. Beller, *Chem. Sci.*, 2020, **11**, 2973–2981.
173 M. Elfinger, T. Schönauer, S. L. J. Thomä, R. Stäglich, M. Drechsler, M. Zobel, J. Senker and R. Kempe, *ChemSusChem*, 2021, **14**, 2360–2366.
174 Z. Yuan, B. Liu, P. Zhou, Z. Zhang and Q. Chi, *J. Catal.*, 2019, **370**, 347–356.
175 T. Mitsudome, M. Sheng, A. Nakata, J. Yamasaki, T. Mizugaki and K. Jitsukawa, *Chem. Sci.*, 2020, **11**, 6682–6689.
176 H. F. Qi, Y. R. Li, Z. T. Zhou, Y. Q. Cao, F. Liu, W. X. Guan, L. L. Zhang, X. Y. Liu, L. Li, Y. Su, K. Junge, X. Z. Duan, M. Beller, A. Q. Wang and T. Zhang, *Nat. Commun.*, 2023, **14**, 6329.
177 W. She, J. Wang, X. Li, J. Li, G. Mao, W. Li and G. Li, *J. Catal.*, 2021, **401**, 17–26.
178 J. Xian, Y. Lin, Z. Sun, Z. Wang, L. Chen, X. Chen, X. Peng and F. Xie, *J. Catal.*, 2024, **439**, 115774.